**Fig. 2**

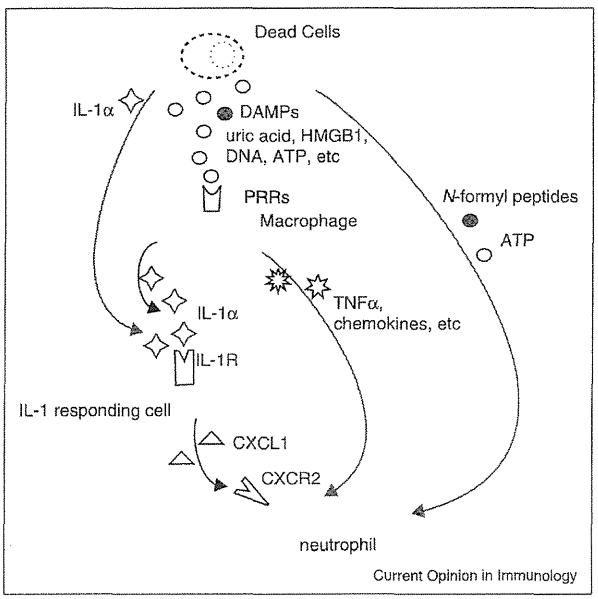


The role of IL-1 in necrotic cell death induced inflammation. Necrotic cells release intracellular contents, some of which act as danger signals (DAMPs). Macrophages at the site of tissue injury recognize DAMPs via Pattern recognition receptors (PRRs) and release IL-1α. IL-1α acts as one of the primary DAMPs when dendritic cells become necrotic. IL-1α then binds the IL-1 receptor (IL-1R) on a non-bone marrow-derived responding cell, resulting in the attraction and activation of neutrophils. IL-1α stimulates the chemoattractant chemokines, that is, CXCL1 and CXCL2, and the receptor CXCR2 expression is required for the neutrophil recruitment. In addition to IL-1 pathway, macrophages also respond to DAMPs to generate chemokines and cytokines including TNFα that leads to neutrophil recruitment. ATP and *N*-formyl peptides directly guides neutrophils to injured cells.

acts as a primary danger signal via the ST2 receptor [20,39]. In other experiments, TLR9 was shown to be responsible for inducing liver toxicity in response to excess amounts of acetaminophen or pancreatitis in response to cerulein [52,53].

Recently, a growing number of receptors that recognize innate cytosolic patterns have been identified; these sense either DNA or RNA, including AIM2, RIG-I, and DAI [54,55]. The setting of compromised DNA hydrolysis, such as DNase deficiency, leads to the development of DNA-driven, IFN-dependent autoimmune diseases [56,57]. Although there is no direct evidence of a role for DNA sensors in cell-death-induced acute inflammation, there is emerging evidence that these cytosolic receptors play a major role in autoimmunity-related inflammation [58] or have adjuvant properties [59,60].

ATP is recognized by the P2X7 and P2Y2 receptors in cell-death-induced inflammation [26,43]. The anti-inflammatory properties of adenosine are mediated by A2A receptor [47•,48,61].

HMGB1 binds to RAGE and TLRs and exerts its function in inflammation [27•,32]. Later it is shown that HMGB1 binds to other molecules including ssDNA, LPS, IL-1β and nucleosomes, which are recognized by TLR9, TLR4, IL-1R, and TLR2 receptors, respectively [62•].

Recent advances in the research in C-type lectin receptors revealed their functions in recognizing danger signals in addition to apoptotic cells or microbial components [63,64]. C type lectin, Lox-1, Mgl1 and DEC205 were known for sensing apoptotic cells. Mincle (Clec4e) is expressed on macrophages and neutrophils that senses SAP130 released from necrotic cells to stimulate inflammation including cytokine production and neutrophil recruitment [65•]. DNGR-1 (Clec9a) is expressed on CD8α+ dendritic cells and promotes cross-presentation of dead cell-associated antigens to activate cytotoxic T lymphocytes [63,66•,67]. Subsequently actin filaments of cytoskeleton were identified as ligand for DNGR-1. Actin filaments which are usually sequestered inside of cells are exposed to extracellular space when cells are damaged [68,69].

To date, no specific receptor for uric acid or MSU crystals working as a danger signal has been identified. Using atomic force microscopy, cholesterol within the plasma membrane was identified as the receptor for MSU crystals [70]. Martinon *et al.* found that the NLRP3 protein, a NOD-like receptor, forms a multi-molecule complex with ASC and caspase-1, named the inflammasome in analogy to the apoptosome [71•]. The inflammasome acts as a platform for activating caspase-1, which results in the maturation of inactive pro IL-1β to active IL-1β. The NLRP3 inflammasome is shown to be required for secretion of IL-1β and neutrophil recruitment *in vivo* [72].

It was initially proposed that pore formation allows extracellular NLRP3 agonists to access the cytosol and activate NLRP3 directly [41,73]. However, the structural diversity of growing number of NLRP3 activators argues against a direct interaction between NLRP3 and all of its activators. Subsequently, Hornung *et al.* presented evidence that NLRP3 senses vesicular rupture, which led to a new concept: NLRP3 monitors cell health and responds to internal cell damage [74]. This is another example of the concept of danger signals fitting inside cells which is analogous to the concept, 'ontogeny recapitulates phylogeny' of Ernst Haeckel. At the level of an organism, the danger signals, usually hidden molecules from the immune system, are released to extracellular milieu when tissues are broken down to evoke the responses. At the cellular level, NLRP3 inflammasome responds to the

intracellular changes that indicate cellular damage, for example, pore formation of plasma membrane, vesicular rupture or cellular stress. It was shown that mitochondrial membrane permeabilization represents the point of no return of programmed cell death pathways that leads to apoptosis or programmed necrosis [75,76]. It is recently shown that mitochondrial dysfunction and ROS production activates NLRP3 inflammasome that is enhanced if mitophagy/autophagy does not kick in appropriately [77,78•,79,80]. In addition, mitochondrial DNA or cardiolipin released to cytosol also induces NLRP3 inflammasome activation [78•,81,82]. These recently added evidences along with the previous ones shed the light on the central role of mitochondria as the central regulator of cellular stress management linking to inflammation. In addition, NLRP3 inflammasome senses internal damage of the cell including the damage of plasma membrane via cytosolic potassium concentration [83] or cell volume [84].

### Sensor cells for danger signals that generate IL-1

As stated above, one of the major recent discoveries in cell-death-induced inflammation is that cytokine IL-1 plays an important role in this response. Since IL-1 is generated and released by cells, studies investigated which cell lineage produces IL-1. Since many cell types can produce this cytokine, we generated chimeric mice whose bone marrow lacked functional IL-1 genes or similar radioresistant parenchyma cells and challenged them with necrotic cells intraperitoneally [37]. Utilizing the CD11b-DTR system and reconstitution, we identified CD11b+ macrophages as the key player sensing cell death and producing IL-1α *in vivo* (Figure 2). Of note, CD11c+ cells also have the ability to reduce inflammation in CD11b-DTR mice. However, in another set of experiments using CD11c-DTR mice in which DT treatment transiently deleted most dendritic cell subsets and the CD11c+ subset of CD8+ T cells, we found that CD11c+ dendritic cells do not play major role in the acute inflammatory response to cell death. Interestingly, macrophages are the major source of IL-1α needed for the cell-death-induced inflammatory response in our models. In addition, IL-1β was required for the cell-death-induced inflammatory response. The dominant source of IL-1β in this response was bone marrow-derived cells. The IL-1α and IL-1β release from macrophages in response to dead cells depends on MAP3K8 (Cot/tpl2) [85]. Macrophages and Kupffer cells were shown to be NLRP3 inflammasome activated and secrete IL-1β in response to necrotic cells [42,86]. Although IL-1α secretion and IL-1β processing is dependent on inflammasome *in vitro*, caspase-1 is not required *in vivo* for much of the IL-1β-dependent sterile inflammatory response [87]. IL-1β is processed by leukocyte serine proteases which are controlled by cathepsin C in the caspase-1 independent pathway [87]. CD8+ dendritic cells recognize necrotic cells via DNGR-1 (Clac9a) to cross present the dead cell associated antigens *in vitro* and *in vivo* [66•]. Monocytes respond to necrotic cells to produce TNF-α [27•]. Another innate immune cell type resident in tissues is mast cells. Mast cells mount an inflammatory response to dead fibroblasts by recognizing the dead-cell-spilling IL-33 as a primary danger signal [20,39]. Eosinophils also participate in the inflammatory responses to necrotic cell-derived danger signals including MSU crystal to secrete cytokines and chemokines, although shown only *in vitro* [26,88].

### Effector cells that recruit neutrophils

IL-1 and the IL-1 receptor pathway are essential for neutrophil recruitment to the site of cell-death-induced inflammation, as described above. CD11b+ macrophages are required to produce IL-1α and bone-marrow-derived cells are required to produce IL-1β. Bone marrow chimeric experiments revealed that the IL-1 receptor is required on parenchymal, non-bone-marrow-derived cells, but not on bone-marrow-derived cells [4••]. These results indicate that neutrophils are recruited to the site of inflammation in a manner other than by recognizing IL-1 on their receptors directly. The neutrophil recruitment is initiated by the activation of adhesion molecules (e.g. ICAM-1) on the endothelium neighboring the injury. In response to necrotic dendritic cells which releases abundant IL-1α that is sensed by the IL-1R on mesothelial cells to induce the production of neutrophil-attracting chemokines (e.g. CXCL1) [18]. Neutrophils transmigrate to the vicinity of the necrotic focus according to the gradient of CXCR2 ligands, such as CXCL1 [18,43].

## Conclusions

A significant progress has been made in revealing the mechanisms underlying the generation of the neutrophilic inflammatory response in response to sterile necrosis. The identification of IL-1 as a key molecule for this process was an important step; and is shared by inflammation to sterile particulates. In addition to the role of NLRP3 inflammasome for IL-1α and IL-1β processing and secretion, new potential players that function in this process have been identified. These findings open the possibility of developing new therapies and therapeutics to treat diseases that are caused by necrotic cell death- or sterile particulates-induced inflammation including myocardial infarction, stroke, drug induced liver injury, SIRS, and NLRP3 inflammasome related diseases including gout, diabetes mellitus and atherosclerosis.

## Acknowledgements

The authors thank Dr. Kenneth L. Rock for numerous input whose many work are cited in the references. This work is supported by a Grant for Research on Intractable Diseases from the Ministry of Health, Labour and Welfare and Grant-in-Aid (C) and Grant-in-Aid for Scientific Research on Innovative Areas for Scientific Research from the Ministry of Education, Culture, Sports, Science, and Technology of Japan. HK is also supported by The Naito Foundation and a rheumatology research grant from Bristol-Myers Squibb.

## References and recommended reading

Papers of particular interest, published within the period of review, have been highlighted as:

- • of special interest
- •• of outstanding interest


1. Rock KL, Latz E, Ontiveros F, Kono H: **The sterile inflammatory response.** *Annu Rev Immunol* 2010, **28**:321-342.

2. Chen GY, Nunez G: **Sterile inflammation: sensing and reacting to damage.** *Nat Rev Immunol* 2010, **10**:826-837.

3. Shen H, Kreisel D, Goldstein DR: **Processes of sterile inflammation.** *J Immunol* 2013, **191**:2857-2863.

4. •• Chen CJ, Kono H, Golenbock D, Reed G, Akira S, Rock KL: **Identification of a key pathway required for the sterile inflammatory response triggered by dying cells.** *Nat Med* 2007, **13**:851-856.

This paper identifies IL-1α as an important molecule to recruit neutrophil to necrotic cells *in vivo*. Also it showed that individual TLRs do not play dominant role in the response.

5. Kurt-Jones EA, Beller DI, Mizel SB, Unanue ER: **Identification of a membrane-associated interleukin 1 in macrophages.** *Proc Natl Acad Sci U S A* 1985, **82**:1204-1208.

6. •• Kuida K, Lippke JA, Ku G, Harding MW, Livingston DJ, Su MS, Flavell RA: **Altered cytokine export and apoptosis in mice deficient in interleukin-1 beta converting enzyme.** *Science* 1995, **267**:2000-2003.

It was known that IL-1α is not a substrate of caspase-1, still this paper showed that caspase-1 is required for secretion of IL-1α, in addition to maturation of IL-1β

7. Dinarello CA: **Immunological and inflammatory functions of the interleukin-1 family.** *Annu Rev Immunol* 2009, **275**:19-550.

8. Miao EA, Rajan JV, Aderem A: **Caspase-1-induced pyroptotic cell death.** *Immunol Rev* 2011, **243**:206-214.

9. Janeway CA Jr: **Approaching the asymptote? Evolution and revolution in immunology.** *Cold Spring Harb Symp Quant Biol* 1989, **54Pt**:11-13.

10. Matzinger P: **Tolerance, danger, and the extended family.** *Annu Rev Immunol* 1994, **12**:991-1045.

11. Gallucci S, Lolkema M, Matzinger P: **Natural adjuvants: endogenous activators of dendritic cells.** *Nat Med* 1999, **5**:1249-1255.

12. Shi Y, Zheng W, Rock KL: **Cell injury releases endogenous adjuvants that stimulate cytotoxic T cell responses.** *Proc Natl Acad Sci U S A* 2000, **97**:14590-14595.

13. Akira S, Uematsu S, Takeuchi O: **Pathogen recognition and innate immunity.** *Cell* 2006, **124**:783-801.

14. Majno G, Joris I: **Apoptosis, oncosis, and necrosis. An overview of cell death.** *Am J Pathol* 1995, **146**:3-15.

15. Majno G, La Gattuta M, Thompson TE: **Cellular death and necrosis: chemical, physical and morphologic changes in rat liver.** *Virchows Arch Pathol Anat Physiol Klin Med* 1960, **333**:421-465.

16. Rock KL, Kono H: **The inflammatory response to cell death.** *Annu Rev Pathol* 2008, **3**:99-126.

17. Rock KL, Lai JJ, Kono H: **Innate and adaptive immune responses to cell death.** *Immunol Rev* 2011, **243**:191-205.

18. Eigenbrod T, Park JH, Harder J, Iwakura Y, Nunez G: **Cutting edge: critical role for mesothelial cells in necrosis-induced inflammation through the recognition of IL-1alpha released from dying cells.** *J Immunol* 2008, **181**:8194-8198.

19. Moussion C, Ortega N, Girard JP: **The IL-1-like cytokine IL-33 is constitutively expressed in the nucleus of endothelial cells and epithelial cells in vivo: a novel 'alarmin'?** *PLoS ONE* 2008, **3**:e3331.

20. Enoksson M, Lyberg K, Moller-Westerberg C, Fallon PG, Nilsson G, Lunderius-Andersson C: **Mast cells as sensors of cell injury through IL-33 recognition.** *J Immunol* 2011, **186**:2523-2528.

21. • Shi Y, Evans JE, Rock KL: **Molecular identification of a danger signal that alerts the immune system to dying cells.** *Nature* 2003, **425**:516-521.

This paper identified uric acid (monosodium urate crystal) as a danger signal to promote cytotoxic T cell response to dead-cell associated antigen.

22. Kono H, Chen CJ, Ontiveros F, Rock KL: **Uric acid promotes an acute inflammatory response to sterile cell death in mice.** *J Clin Invest* 2010, **120**:1939-1949.

23. Gasse P, Riteau N, Charron S, Girre S, Fick L, Petrilli V, Tschopp J, Lagente V, Quesniaux VF, Ryffel B *et al.*: **Uric acid is a danger signal activating NALP3 inflammasome in lung injury inflammation and fibrosis.** *Am J Respir Crit Care Med* 2009, **179**:903-913.

24. Zhou Y, Fang L, Jiang L, Wen P, Cao H, He W, Dai C, Yang J: **Uric acid induces renal inflammation via activating tubular NF-kappaB signaling pathway.** *PLoS One* 2012, **7**:e39738.

25. McCarty DJ, Hollander JL: **Identification of urate crystals in gouty synovial fluid.** *Ann Int Med* 1961, **54**:452.

26. Kobayashi T, Kouzaki H, Kita H: **Human eosinophils recognize endogenous danger signal crystalline uric acid and produce proinflammatory cytokines mediated by autocrine ATP.** *J Immunol* 2010, **184**:6350-6358.

27. • Scaffidi P, Misteli T, Bianchi ME: **Release of chromatin protein HMGB1 by necrotic cells triggers inflammation.** *Nature* 2002, **418**:191-195.

This paper identified HMGB1 as a danger signal released from necrotic cell but not from apoptotic cells, and induce acute inflammation.

28. Andersson U, Erlandsson-Harris H, Yang H, Tracey KJ: **HMGB1 as a DNA-binding cytokine.** *J Leukoc Biol* 2002, **72**:1084-1091.

29. Bianchi ME: **DAMPs PAMPs and alarmins: all we need to know about danger.** *J Leukoc Biol* 2007, **81**:1-5.

30. Andersson U, Wang H, Palmblad K, Aveberger AC, Bloom O, Erlandsson-Harris H, Janson A, Kokkola R, Zhang M, Yang H *et al.*: **High mobility group 1 protein (HMG-1) stimulates proinflammatory cytokine synthesis in human monocytes.** *J Exp Med* 2000, **192**:565-570.

31. Rouhiainen A, Tumova S, Valmu L, Kalkkinen N, Rauvala H: **Analysis of proinflammatory activity of highly purified eukaryotic recombinant HMGB1 (amphoterin).** *J Leukoc Biol* 2007, **81**:49-58.

32. Tian J, Avalos AM, Mao SY, Chen B, Senthil K, Wu H, Parroche P, Drabic S, Golenbock D, Sirois C *et al.*: **Toll-like receptor 9-dependent activation by DNA-containing immune complexes is mediated by HMGB1 and RAGE.** *Nat Immunol* 2007, **8**:487-496.

33. Sha Y, Zmijewski J, Xu Z, Abraham E: **HMGB1 develops enhanced proinflammatory activity by binding to cytokines.** *J Immunol* 2008, **180**:2531-2537.

34. Krysko DV, Agostinis P, Krysko O, Garg AD, Bachert C, Lambrecht BN, Vandenabeele P: **Emerging role of damage-associated molecular patterns derived from mitochondria in inflammation.** *Trends Immunol* 2011, **32**:157-164.

35. Clarke MC, Talib S, Figg NL, Bennett MR: **Vascular smooth muscle cell apoptosis induces interleukin-1-directed inflammation: effects of hyperlipidemia-mediated inhibition of phagocytosis.** *Circ Res* 2010, **106**:363-372.

36. Cohen I, Rider P, Carmi Y, Braiman A, Dotan S, White MR, Voronov E, Martin MU, Dinarello CA, Apte RN: **Differential release of chromatin-bound IL-1alpha discriminates between necrotic and apoptotic cell death by the ability to induce sterile inflammation.** *Proc Natl Acad Sci U S A* 2010, **107**:2574-2579.

37. Kono H, Karmarkar D, Iwakura Y, Rock KL: **Identification of the cellular sensor that stimulates the inflammatory response to sterile cell death.** *J Immunol* 2010, **184**:4470-4478.

38. • Zheng Y, Humphry M, Maguire JJ, Bennett MR, Clarke MC: **Intracellular interleukin-1 receptor 2 binding prevents**

**cleavage and activity of interleukin-1alpha, controlling necrosis-induced sterile inflammation.** *Immunity* 2013, **38**:285-295.
This paper identifies Intracellular interleukin-1 receptor 2 as a negative regulator for IL-1αspilling from dead cell as a primary danger signal.

39. Enoksson M, Moller-Westerberg C, Wicher G, Fallon PG, Forsberg-Nilsson K, Lunderius-Andersson C, Nilsson G: **Intraperitoneal influx of neutrophils in response to IL-33 is mast cell-dependent.** *Blood* 2013, **121**:530-536.

40. Kahlenberg JM, Dubyak GR: **Mechanisms of caspase-1 activation by P2X7 receptor-mediated K+ release.** *Am J Physiol Cell Physiol* 2004, **286**:C1100-C1108.

41. Kanneganti TD, Lamkanfi M, Kim YG, Chen G, Park JH, Franchi L, Vandenabeele P, Nunez G: **Pannexin-1-mediated recognition of bacterial molecules activates the cryopyrin inflammasome independent of Toll-like receptor signaling.** *Immunity* 2007, **26**:433-443.

42. Iyer SS, Pulskens WP, Sadler JJ, Butter LM, Teske GJ, Ulland TK, Eisenbarth SC, Florquin S, Flavell RA, Leemans JC *et al.*: **Necrotic cells trigger a sterile inflammatory response through the Nlrp3 inflammasome.** *Proc Natl Acad Sci U S A* 2009, **106**:20388-20393.

43. McDonald B, Pittman K, Menezes GB, Hirota SA, Slaba I, Waterhouse CC, Beck PL, Muruve DA, Kubes P: **Intravascular danger signals guide neutrophils to sites of sterile inflammation.** *Science* 2010, **330**:362-366.

44. • Elliott MR, Chekeni FB, Trampont PC, Lazarowski ER, Kadl A, Walk SF, Park D, Woodson RI, Ostankovich M, Sharma P *et al.*: **Nucleotides released by apoptotic cells act as a find-me signal to promote phagocytic clearance.** *Nature* 2009, **461**:282-286.
This paper showed that ATP and UTP are released from apoptotic cells that signal through $P2Y_2$ receptors and act as 'find-me' signal to recruit monocytes.

45. Ravichandran KS: **Find-me and eat-me signals in apoptotic cell clearance: progress and conundrums.** *J Exp Med* 2010, **207**:1807-1817.

46. Sitkovsky MV, Ohta A: **The 'danger' sensors that STOP the immune response: the A2 adenosine receptors?** *Trends Immunol* 2005, **26**:299-304.

47. • Ohta A, Sitkovsky M: **Role of G-protein-coupled adenosine receptors in downregulation of inflammation and protection from tissue damage.** *Nature* 2001, **414**:916-920.
This paper identify adenosine as a molecule released from dead cell to terminate the inflammation through A2A adenosine receptor.

48. Day YJ, Marshall MA, Huang L, McDuffie MJ, Okusa MD, Linden J: **Protection from ischemic liver injury by activation of A2A adenosine receptors during reperfusion: inhibition of chemokine induction.** *Am J Physiol Gastrointest Liver Physiol* 2004, **286**:G285-G293.

49. Matzinger P, Kamala T: **Tissue-based class control: the other side of tolerance.** *Nat Rev Immunol* 2011, **11**:221-230.

50. Akira S, Takeda K: **Toll-like receptor signalling.** *Nat Rev Immunol* 2004, **4**:499-511.

51. Kaisho T, Akira S: **Toll-like receptor function and signaling.** *J Allergy Clin Immunol* 2006, **117**:979-987 quiz 988.

52. Imaeda AB, Watanabe A, Sohail MA, Mahmood S, Mohamadnejad M, Sutterwala FS, Flavell RA, Mehal WZ: **Acetaminophen-induced hepatotoxicity in mice is dependent on Tlr9 and the Nalp3 inflammasome.** *J Clin Invest* 2009, **119**:305-314.

53. Hoque R, Sohail M, Malik A, Sarwar S, Luo Y, Shah A, Barrat F, Flavell R, Gorelick F, Husain S *et al.*: **TLR9 and the NLRP3 inflammasome link acinar cell death with inflammation in acute pancreatitis.** *Gastroenterology* 2011, **141**:358-369.

54. Rathinam VA, Fitzgerald KA: **Cytosolic surveillance and antiviral immunity.** *Curr Opin Virol* 2011, **1**:455-462.

55. Broz P, Monack DM: **Newly described pattern recognition receptors team up against intracellular pathogens.** *Nat Rev Immunol* 2013, **13**:551-565.

56. Yoshida H, Okabe Y, Kawane K, Fukuyama H, Nagata S: **Lethal anemia caused by interferon-beta produced in mouse embryos carrying undigested DNA.** *Nat Immunol* 2005, **6**:49-56.

57. Stetson DB, Ko JS, Heidmann T, Medzhitov R: **Trex1 prevents cell-intrinsic initiation of autoimmunity.** *Cell* 2008, **134**:587-598.

58. Ahn J, Gutman D, Saijo S, Barber GN: **STING manifests self DNA-dependent inflammatory disease.** *Proc Natl Acad Sci U S A* 2012, **109**:19386-19391.

59. Ishii KJ, Kawagoe T, Koyama S, Matsui K, Kumar H, Kawai T, Uematsu S, Takeuchi O, Takeshita F, Coban C *et al.*: **TANK-binding kinase-1 delineates innate and adaptive immune responses to DNA vaccines.** *Nature* 2008, **451**:725-729.

60. Kis-Toth K, Szanto A, Thai TH, Tsokos GC: **Cytosolic DNA-activated human dendritic cells are potent activators of the adaptive immune response.** *J Immunol* 2011, **187**:1222-1234.

61. Lukashev D, Ohta A, Apasov S, Chen JF, Sitkovsky M: **Cutting edge: physiologic attenuation of proinflammatory transcription by the Gs protein-coupled A2A adenosine receptor in vivo.** *J Immunol* 2004, **173**:21-24.

62. • Bianchi ME: **HMGB1 loves company.** *J Leukoc Biol* 2009, **86**:573-576.
This review paper clarifies the current understanding of HMGB1 as a binding partner to multiple danger signals to interact with RAGE along with the receptor for the partners.

63. Iborra S, Izquierdo HM, Martinez-Lopez M, Blanco-Menendez N, Reis e Sousa C, Sancho D: **The DC receptor DNGR-1 mediates cross-priming of CTLs during vaccinia virus infection in mice.** *J Clin Invest* 2012, **122**:1628-1643.

64. Sancho D, Reis e Sousa C: **Signaling by myeloid C-type lectin receptors in immunity and homeostasis.** *Annu Rev Immunol* 2012, **30**:491-529.

65. • Yamasaki S, Ishikawa E, Sakuma M, Hara H, Ogata K, Saito T: **Mincle is an ITAM-coupled activating receptor that senses damaged cells.** *Nat Immunol* 2008, **9**:1179-1188.
This paper shows that SAP-130 is released from necrotic cells and recognized C-type lectin receptor Mincle (Clec9a).

66. • Sancho D, Joffre OP, Keller AM, Rogers NC, Martinez D, Hernanz-Falcon P, Rosewell I, Reis e Sousa C: **Identification of a dendritic cell receptor that couples sensing of necrosis to immunity.** *Nature* 2009, **458**:899-903.
Together with ref 65, these papers highlight the importance of C-type lectin receptor for danger signals. This paper identifies DNGR-1 as a DC receptor for sensing necrotic cells. DNGR-1 is essential for MHC class I cross-presentation of dead-cell associated antigens.

67. Zelenay S, Keller AM, Whitney PG, Schraml BU, Deddouche S, Rogers NC, Schulz O, Sancho D, Reis e Sousa C: **The dendritic cell receptor DNGR-1 controls endocytic handling of necrotic cell antigens to favor cross-priming of CTLs in virus-infected mice.** *J Clin Invest* 2012, **122**:1615-1627.

68. Zhang JG, Czabotar PE, Policheni AN, Caminschi I, Wan SS, Kitsoulis S, Tullett KM, Robin AY, Brammananth R, van Delft MF *et al.*: **The dendritic cell receptor Clec9A binds damaged cells via exposed actin filaments.** *Immunity* 2012, **36**:646-657.

69. Ahrens S, Zelenay S, Sancho D, Hanc P, Kjaer S, Feest C, Fletcher G, Durkin C, Postigo A, Skehel M *et al.*: **F-actin is an evolutionarily conserved damage-associated molecular pattern recognized by DNGR-1, a receptor for dead cells.** *Immunity* 2012, **36**:635-645.

70. Ng G, Sharma K, Ward SM, Desrosiers MD, Stephens LA, Schoel WM, Li T, Lowell CA, Ling CC, Amrein MW *et al.*: **Receptor-independent, direct membrane binding leads to cell-surface lipid sorting and Syk kinase activation in dendritic cells.** *Immunity* 2008, **29**:807-818.

71. • Martinon F, Burns K, Tschopp J: **The inflammasome: a molecular platform triggering activation of inflammatory caspases and processing of proIL-beta.** *Mol Cell* 2002, **10**:417-426.
This paper identified the multimolecular platform inflammasome for caspase-1 activation and il-1β cleavage.

72. Martinon F, Petrilli V, Mayor A, Tardivel A, Tschopp J: **Gout-associated uric acid crystals activate the NALP3 inflammasome.** *Nature* 2006, **440**:237-241.

73. Chen GJ, Shi Y, Hearn A, Fitzgerald K, Golenbock D, Reed G, Akira S, Rock KL: **MyD88-dependent IL-1 receptor signaling is essential for gouty inflammation stimulated by monosodium urate crystals.** *J Clin Invest* 2006, **116**:2262-2271.

74. Hornung V, Bauernfeind F, Halle A, Samstad EO, Kono H, Rock KL, Fitzgerald KA, Latz E: **Silica crystals and aluminum salts activate the NALP3 inflammasome through phagosomal destabilization.** *Nat Immunol* 2008, **9**:847-856.

75. Kroemer G, Galluzzi L, Brenner C: **Mitochondrial membrane permeabilization in cell death.** *Physiol Rev* 2007, **87**:99-163.

76. Baines CP: **Role of the mitochondrion in programmed necrosis.** *Front Physiol* 2010, **1**:156.

77. Zhou R, Yazdi AS, Menu P, Tschopp J: **A role for mitochondria in NLRP3 inflammasome activation.** *Nature* 2011, **469**:221-225.

78. • Nakahira K, Haspel JA, Rathinam VA, Lee SJ, Dolinay T, Lam HC, Englert JA, Rabinovitch M, Cernadas M, Kim HP *et al.*: **Autophagy proteins regulate innate immune responses by inhibiting the release of mitochondrial DNA mediated by the NALP3 inflammasome.** *Nat Immunol* 2011, **12**:222-230.
This paper confirms the close link between autophagy and inflammasome. The failure in autophagy results in releaseing mitochondria DNA to cytosol which results in NLRP3 inflammasome activation.

79. Heid ME, Keyel PA, Kamga C, Shiva S, Watkins SC, Salter RD: **Mitochondrial reactive oxygen species induces nlrp3-dependent lysosomal damage and inflammasome activation.** *J Immunol* 2013, **191**:5230-5238.

80. Park S, Juliana C, Hong S, Datta P, Hwang I, Fernandes-Alnemri T, Yu JW, Alnemri ES: **The mitochondrial antiviral protein MAVS associates with NLRP3 and regulates its inflammasome activity.** *J Immunol* 2013, **191**:4358-4366.

81. Shimada K, Crother TR, Karlin J, Dagvadorj J, Chiba N, Chen S, Ramanujan VK, Wolf AJ, Vergnes L, Ojcius DM *et al.*: **Oxidized mitochondrial DNA activates the NLRP3 inflammasome during apoptosis.** *Immunity* 2012, **36**:401-414.

82. Iyer SS, He Q, Janczy JR, Elliott EI, Zhong Z, Olivier AK, Sadler JJ, Knepper-Adrian V, Han R, Qiao L *et al.*: **Mitochondrial cardiolipin is required for Nlrp3 inflammasome activation.** *Immunity* 2013, **39**:311-323.

83. Petrilli V, Papin S, Dostert C, Mayor A, Martinon F, Tschopp J: **Activation of the NALP3 inflammasome is triggered by low intracellular potassium concentration.** *Cell Death Differ* 2007, **14**:1583-1589.

84. Wen H, Miao EA, Ting JP: **Mechanisms of NOD-like receptor-associated inflammasome activation.** *Immunity* 2013, **39**:432-441.

85. Sanz-Garcia C, Ferrer-Mayorga G, Gonzalez-Rodriguez A, Valverde AM, Martin-Duce A, Velasco-Martin JP, Regadera J, Fernandez M, Alemany S: **Sterile inflammation in acetaminophen-induced liver injury is mediated by Cot/tpl2.** *J Biol Chem* 2013, **288**:15342-15351.

86. Huang H, Chen HW, Evankovich J, Yan W, Rosborough BR, Nace GW, Ding Q, Loughran P, Beer-Stolz D, Billiar TR *et al.*: **Histones activate the NLRP3 inflammasome in Kupffer cells during sterile inflammatory liver injury.** *J Immunol* 2013, **191**:2665-2679.

87. Kono H, Orlowski GM, Patel Z, Rock KL: **The IL-1-dependent sterile inflammatory response has a substantial caspase-1-independent component that requires cathepsin C.** *J Immunol* 2012, **189**:3734-3740.

88. Stenfeldt AL, Wenneras C: ***Danger signals derived from* stressed and necrotic epithelial cells activate human eosinophils.** *Immunology* 2004, **112**:605-614.

89. Hori O, Brett J, Slattery T, Cao R, Zhang J, Chen JX, Nagashima M, Lundh ER, Vijay S, Nitecki D *et al.*: **The receptor for advanced glycation end products (RAGE) is a cellular binding site for amphoterin. Mediation of neurite outgrowth and co-expression of rage and amphoterin in the developing nervous system.** *J Biol Chem* 1995, **270**:25752-25761.

90. Andrassy M, Volz HC, Igwe JC, Funke B, Eichberger SN, Kaya Z, Buss S, Autschbach F, Pleger ST, Lukic IK *et al.*: **High-mobility group box-1 in ischemia-reperfusion injury of the heart.** *Circulation* 2008, **117**:3216-3226.

91. Degryse B, Bonaldi T, Scaffidi P, Muller S, Resnati M, Sanvito F, Arrigoni G, Bianchi ME: **The high mobility group (HMG) boxes of the nuclear protein HMG1 induce chemotaxis and cytoskeleton reorganization in rat smooth muscle cells.** *J Cell Biol* 2001, **152**:1197-1206.

92. Hofmann MA, Drury S, Fu C, Qu W, Taguchi A, Lu Y, Avila C, Kambham N, Bierhaus A, Nawroth P *et al.*: **RAGE mediates a novel proinflammatory axis: a central cell surface receptor for S100/calgranulin polypeptides.** *Cell* 1999, **97**:889-901.

93. Rovere-Querini P, Capobianco A, Scaffidi P, Valentinis B, Catalanotti F, Giazzon M, Dumitriu IE, Muller S, Iannacone M, Traversari C *et al.*: **HMGB1 is an endogenous immune adjuvant released by necrotic cells.** *EMBO Rep* 2004, **5**:825-830.

94. Messmer D, Yang H, Telusma G, Knoll F, Li J, Messmer B, Tracey KJ, Chiorazzi N: **High mobility group box protein 1: an endogenous signal for dendritic cell maturation and Th1 polarization.** *J Immunol* 2004, **173**:307-313.

95. Chavakis E, Hain A, Vinci M, Carmona G, Bianchi ME, Vajkoczy P, Zeiher AM, Chavakis T, Dimmeler S: **High-mobility group box 1 activates integrin-dependent homing of endothelial progenitor cells.** *Circ Res* 2007, **100**:204-212.

96. Apetoh L, Ghiringhelli F, Tesniere A, Obeid M, Ortiz C, Criollo A, Mignot G, Maiuri MC, Ullrich E, Saulnier P *et al.*: **Toll-like receptor 4-dependent contribution of the immune system to anticancer chemotherapy and radiotherapy.** *Nat Med* 2007, **13**:1050-1059.

97. Tsung A, Sahai R, Tanaka H, Nakao A, Fink MP, Lotze MT, Yang H, Li J, Tracey KJ, Geller DA *et al.*: **The nuclear factor HMGB1 mediates hepatic injury after murine liver ischemia-reperfusion.** *J Exp Med* 2005, **201**:1135-1143.

98. Kokkola R, Li J, Sundberg E, Aveberger AC, Palmblad K, Yang H, Tracey KJ, Andersson U, Harris HE: **Successful treatment of collagen-induced arthritis in mice and rats by targeting extracellular high mobility group box chromosomal protein 1 activity.** *Arthritis Rheum* 2003, **48**:2052-2058.

99. Muhammad S, Barakat W, Stoyanov S, Murikinati S, Yang H, Tracey KJ, Bendszus M, Rossetti G, Nawroth PP, Bierhaus A *et al.*: **The HMGB1 receptor RAGE mediates ischemic brain damage.** *J Neurosci* 2008, **28**:12023-12031.

100. Shichita T, Hasegawa E, Kimura A, Morita R, Sakaguchi R, Takada I, Sekiya T, Ooboshi H, Kitazono T, Yanagawa T *et al.*: **Peroxiredoxin family proteins are key initiators of post-ischemic inflammation in the brain.** *Nat Med* 2012, **18**:911-917.

101. Kohno T, Anzai T, Kaneko H, Sugano Y, Shimizu H, Shimoda M, Miyasho T, Okamoto M, Yokota H, Yamada S *et al.*: **High-mobility group box 1 protein blockade suppresses development of abdominal aortic aneurysm.** *J Cardiol* 2012, **59**:299-306.

102. Wang H, Bloom O, Zhang M, Vishnubhakat JM, Ombrellino M, Che J, Frazier A, Yang H, Ivanova S, Borovikova L *et al.*: **HMG-1 as a late mediator of endotoxin lethality in mice.** *Science* 1999, **285**:248-251.

103. Liu-Bryan R, Scott P, Sydlaske A, Rose DM, Terkeltaub R: **Innate immunity conferred by Toll-like receptors 2 and 4 and myeloid differentiation factor 88 expression is pivotal to monosodium urate monohydrate crystal-induced inflammation.** *Arthritis Rheum* 2005, **52**:2936-2946.

104. Scott P, Ma H, Viriyakosol S, Terkeltaub R, Liu-Bryan R: **Engagement of CD14 mediates the inflammatory potential of monosodium urate crystals.** *J Immunol* 2006, **177**:6370-6378.

105. Conforti-Andreoni C, Spreafico R, Qian HL, Riteau N, Ryffel B, Ricciardi-Castagnoli P, Mortellaro A: **Uric acid-driven Th17 differentiation requires inflammasome-derived IL-1 and IL-18.** *J Immunol* 2011, **187**:5842-5850.

106. Gordon TP, Kowanko IC, James M, Roberts-Thomson PJ: **Monosodium urate crystal-induced prostaglandin synthesis in the rat subcutaneous air pouch.** *Clin Exp Rheumatol* 1985, **3**:291-296.

107. Terkeltaub R: **Pathogenesis and treatment of crystal-induced inflammation.** In *Arthritis and Allied Conditions*, edn 15th. Edited by Koopman W, Moreland LW.Lippincott Williams and Wilkins; 2005:2357.

108. Shimada M, Johnson RJ, May WS Jr, Lingegowda V, Sood P, Nakagawa T, Van QC, Dass B, Ejaz AA: **A novel role for uric acid in acute kidney injury associated with tumour lysis syndrome.** *Nephrol Dial Transplant* 2009, **24**:2960-2964.

109. Denoble AE, Huffman KM, Stabler TV, Kelly SJ, Hershfield MS, McDaniel GE, Coleman RE, Kraus VB: **Uric acid is a danger signal of increasing risk for osteoarthritis through inflammasome activation.** *Proc Natl Acad Sci U S A* 2011, **108**:2088-2093.

110. Xu J, Zhang X, Monestier M, Esmon NL, Esmon CT: **Extracellular histones are mediators of death through TLR2 and TLR4 in mouse fatal liver injury.** *J Immunol* 2011, **187**:2626-2631.

111. Leadbetter EA, Rifkin IR, Hohlbaum AM, Beaudette BC, Shlomchik MJ, Marshak-Rothstein A: **Chromatin-IgG complexes activate B cells by dual engagement of IgM and Toll-like receptors.** *Nature* 2002, **416**:603-607.

112. Boule MW, Broughton C, Mackay F, Akira S, Marshak-Rothstein A, Rifkin IR: **Toll-like receptor 9-dependent and -independent dendritic cell activation by chromatin-immunoglobulin G complexes.** *J Exp Med* 2004, **199**:1631-1640.

113. Sirois CM, Jin T, Miller AL, Bertheloot D, Nakamura H, Horvath GL, Mian A, Jiang J, Schrum J, Bossaller L *et al.*: **RAGE is a nucleic acid receptor that promotes inflammatory responses to DNA.** *J Exp Med* 2013, **210**:2447-2463.

114. Hornung V, Latz E: **Intracellular DNA recognition.** *Nat Rev Immunol* 2010, **10**:123-130.

115. Bernard JJ, Cowing-Zitron C, Nakatsuji T, Muehleisen B, Muto J, Borkowski AW, Martinez L, Greidinger EL, Yu BD, Gallo RL: **Ultraviolet radiation damages self noncoding RNA and is detected by TLR3.** *Nat Med* 2012, **18**:1286-1290.

116. Hefeneider SH, Cornell KA, Brown LE, Bakke AC, McCoy SL, Bennett RM: **Nucleosomes and DNA bind to specific cell-surface molecules on murine cells and induce cytokine production.** *Clin Immunol Immunopathol* 1992, **63**:245-251.

117. Ishii KJ, Suzuki K, Coban C, Takeshita F, Itoh Y, Matoba H, Kohn LD, Klinman DM: **Genomic DNA released by dying cells induces the maturation of APCs.** *J Immunol* 2001, **167**:2602-2607.

118. Decker P, Singh-Jasuja H, Haager S, Kötter I, Rammensee HG: **Nucleosome, the main autoantigen in systemic lupus erythematosus, induces direct dendritic cell activation via a MyD88-independent pathway: consequences on inflammation.** *J Immunol* 2005, **174**:3326-3334.

119. Ronnefarth VM, Erbacher AI, Lamkemeyer T, Madlung J, Nordheim A, Rammensee HG, Decker P: **TLR2/TLR4-independent neutrophil activation and recruitment upon endocytosis of nucleosomes reveals a new pathway of innate immunity in systemic lupus erythematosus.** *J Immunol* 2006, **177**:7740-7749.

120. Xu J, Zhang X, Pelayo R, Monestier M, Ammollo CT, Semeraro F, Taylor FB, Esmon NL, Lupu F, Esmon CT: **Extracellular histones are major mediators of death in sepsis.** *Nat Med* 2009, **15**:1318-1321.

121. Kaczorowski DJ, Scott MJ, Pibris JP, Afrazi A, Nakao A, Edmonds RD, Kim S, Kwak JH, Liu Y, Fan J *et al.*: **Mammalian DNA is an endogenous danger signal that stimulates local synthesis and release of complement factor B.** *Mol Med* 2012, **18**:851-860.

122. Nicodeme E, Jeffrey KL, Schaefer U, Beinke S, Dewell S, Chung CW, Chandwani R, Marazzi I, Wilson P, Coste H *et al.*: **Suppression of inflammation by a synthetic histone mimic.** *Nature* 2010, **468**:1119-1123.

123. Burnstock G, Knight GE: **Cellular distribution and functions of P2 receptor subtypes in different systems.** *Int Rev Cytol* 2004, **240**:31-304.

124. Mariathasan S, Monack DM: **Inflammasome adaptors and sensors: intracellular regulators of infection and inflammation.** *Nat Rev Immunol* 2007, **7**:31-40.

125. Cronstein BN, Daguma L, Nichols D, Hutchison AJ, Williams M: **The adenosine/neutrophil paradox resolved: human neutrophils possess both A1 and A2 receptors that promote chemotaxis and inhibit O2 generation, respectively.** *J Clin Invest* 1990, **85**:1150-1157.

126. Zhang M, Alicot EM, Chiu I, Li J, Verna N, Vorup-Jensen T, Kessler B, Shimaoka M, Chan R, Friend D *et al.*: **Identification of the target self-antigens in reperfusion injury.** *J Exp Med* 2006, **203**:141-152.

127. Zhang M, Takahashi K, Alicot EM, Vorup-Jensen T, Kessler B, Thiel S, Jensenius JC, Ezekowitz RA, Moore FD, Carroll MC: **Activation of the lectin pathway by natural IgM in a model of ischemia/reperfusion injury.** *J Immunol* 2006, **177**:4727-4734.

128. Weiser MR, Williams JP, Moore FD Jr, Kobzik L, Ma M, Hechtman HB, Carroll MC: **Reperfusion injury of ischemic skeletal muscle is mediated by natural antibody and complement.** *J Exp Med* 1996, **183**:2343-2348.

129. Zhang M, Austen WG Jr, Chiu I, Alicot EM, Hung R, Ma M, Verna N, Xu M, Hechtman HB, Moore FD Jr *et al.*: **Identification of a specific self-reactive IgM antibody that initiates intestinal ischemia/reperfusion injury.** *Proc Natl Acad Sci U S A* 2004, **101**:3886-3891.

130. Fu H, Karlsson J, Bylund J, Movitz C, Karlsson A, Dahlgren C: **Ligand recognition and activation of formyl peptide receptors in neutrophils.** *J Leukoc Biol* 2006, **79**:247-256.

131. Carp H: **Mitochondrial N-formylmethionyl proteins as chemoattractants for neutrophils.** *J Exp Med* 1982, **155**: 264-275.

132. Hauser CJ, Sursal T, Rodriguez EK, Appleton PT, Zhang Q, Itagaki K: **Mitochondrial damage associated molecular patterns from femoral reamings activate neutrophils through formyl peptide receptors and P44/42 MAP kinase.** *J Orthop Trauma* 2010, **24**:534-538.

133. Gawlowski DM, Benoit JN, Granger HJ: **Microvascular pressure and albumin extravasation after leukocyte activation in hamster cheek pouch.** *Am J Physiol* 1993, **264**:H541-H546.

134 • Zhang Q, Raoof M, Chen Y, Sumi Y, Sursal T, Junger W, Brohi K, Itagaki K, Hauser CJ: **Circulating mitochondrial DAMPs cause inflammatory responses to injury.** *Nature* 2010, **464**:104-107.
Mitochondria are evolutionary endosymbionts that were derived from bacteria. This paper identified that mitochondria as a source for danger signals including mitochondria DNA and N-formyl peptides.

135. Marques PE, Amaral SS, Pires DA, Nogueira LL, Soriani FM, Lima BH, Lopes GA, Russo RC, Avila TV, Melgaco JG *et al.*: **Chemokines and mitochondrial products activate neutrophils to amplify organ injury during mouse acute liver failure.** *Hepatology* 2012, **56**:1971-1982.

136. Oka T, Hikoso S, Yamaguchi O, Taneike M, Takeda T, Tamai T, Oyabu J, Murakawa T, Nakayama H, Nishida K *et al.*: **Mitochondrial DNA that escapes from autophagy causes inflammation and heart failure.** *Nature* 2012, **485**:251-255.

137. Julian MW, Shao G, Bao S, Knoell DL, Papenfuss TL, VanGundy ZC, Crouser ED: **Mitochondrial transcription factor A serves as a danger signal by augmenting plasmacytoid dendritic cell responses to DNA.** *J Immunol* 2012, **189**:433-443.

138. Oboki K, Ohno T, Kajiwara N, Arae K, Morita H, Ishii A, Nambu A, Abe T, Kiyonari H, Matsumoto K *et al.*: **IL-33 is a crucial amplifier of innate rather than acquired immunity.** *Proc Natl Acad Sci U S A* 2010, **107**:18581-18586.

nature immunology

# High-density lipoprotein mediates anti-inflammatory reprogramming of macrophages via the transcriptional regulator ATF3

Dominic De Nardo[1,17], Larisa I Labzin[1,17], Hajime Kono[2], Reiko Seki[3], Susanne V Schmidt[4], Marc Beyer[4], Dakang Xu[5,6], Sebastian Zimmer[7], Catharina Lahrmann[7], Frank A Schildberg[8], Johanna Vogelhuber[1], Michael Kraut[4], Thomas Ulas[4], Anja Kerksiek[9], Wolfgang Krebs[4], Niklas Bode[7], Alena Grebe[1], Michael L Fitzgerald[10], Nicholas J Hernandez[10], Bryan R G Williams[5], Percy Knolle[8,11], Manfred Kneilling[12,13], Martin Röcken[12], Dieter Lütjohann[9], Samuel D Wright[14], Joachim L Schultze[4,17] & Eicke Latz[1,15–17]

**High-density lipoprotein (HDL) mediates reverse cholesterol transport and is known to be protective against atherosclerosis. In addition, HDL has potent anti-inflammatory properties that may be critical for protection against other inflammatory diseases. The molecular mechanisms of how HDL can modulate inflammation, particularly in immune cells such as macrophages, remain poorly understood. Here we identify the transcriptional regulator ATF3, as an HDL-inducible target gene in macrophages that downregulates the expression of Toll-like receptor (TLR)-induced proinflammatory cytokines. The protective effects of HDL against TLR-induced inflammation were fully dependent on ATF3 *in vitro* and *in vivo*. Our findings may explain the broad anti-inflammatory and metabolic actions of HDL and provide the basis for predicting the success of new HDL-based therapies.**



The innate immune system uses several families of signaling receptors to detect invading pathogens or tissue damage[1]. Although an appropriate inflammatory response is critical for clearing pathogens and maintaining tissue integrity, excessive or prolonged inflammation can lead to harmful systemic inflammation and organ dysfunction. However, multiple regulatory mechanisms have evolved to limit the extent and duration of the inflammatory response. For instance, activation of TLRs leads to expression of proinflammatory cytokines and also induces expression of many negative regulators, which limit signal transduction, mRNA transcription or translation[2]. Of these, ATF3 is a key inducible transcriptional regulator, which binds to CREB-ATF binding sites in promoters of specific target genes, resulting in chromatin remodeling and subsequent inhibition of transcription-factor binding[3]. ATF3 is induced by TLR stimulation as well as a multitude of other stimuli[4] and acts in a negative-feedback system to limit excessive production of proinflammatory cytokines including TNF, IL-6 and IL-12p40 (refs. 3,5). Understanding how these regulatory pathways function in the context of chronic inflammatory disease is of great interest and may lead to the design of beneficial therapeutics.

Atherosclerosis is the chronic inflammatory condition underlying coronary artery disease and is driven in part via the recognition of metabolic danger signals by innate immune receptors on macrophages[6,7]. Elevated levels of HDL cholesterol are associated with reduced atherothrombotic events[8]. Furthermore, studies in animals have shown HDL to be beneficial on the key cell types and processes in atherosclerosis, in part by mediating the removal of cholesterol from lipid-laden macrophages (known as foam cells)[9]. However, therapies based on simply increasing amounts of HDL have been largely unsuccessful[10,11], prompting the suggestion that the functionality of HDL may be more important to disease outcome than the quantity of HDL itself[12]. Indeed, cholesterol efflux capacity is better correlated with disease risk than the total amount of HDL cholesterol[13]. HDL also has antioxidant, antithrombotic and anti-inflammatory properties, which may also protect against atherogenesis[14–16]. The anti-inflammatory nature of HDL could also be beneficial in other inflammatory diseases: it can lower expression of endothelial cell vascular cell adhesion molecule 1 (VCAM-1), increase production of endothelial nitric oxide synthase (eNOS) and reduce expression of monocyte CD11b and

[1]Institute of Innate Immunity, University Hospitals, Biomedical Centre, University of Bonn, Bonn, Germany. [2]Department of Internal Medicine, Teikyo University School of Medicine, Tokyo, Japan. [3]Department of Clinical Laboratory Science, Teikyo University Faculty of Medical Technology, Tokyo, Japan. [4]Life and Medical Sciences Institute, University of Bonn, Bonn, Germany. [5]Monash Institute of Medical Research, Monash University, Melbourne, Victoria, Australia. [6]Institute of Ageing Research, Hangzhou Normal University School of Medicine, Hangzhou, China. [7]Department of Medicine/Cardiology, University of Bonn, Bonn, Germany. [8]Institutes of Molecular Medicine and Experimental Immunology, University of Bonn, Bonn, Germany. [9]Institute for Clinical Chemistry and Clinical Pharmacology, University of Bonn, Bonn, Germany. [10]Lipid Metabolism Unit, Massachusetts General Hospital, Harvard Medical School, Boston, Massachusetts, USA. [11]Institute of Molecular Immunology, Technical University of Munich, Munich, Germany. [12]Department of Dermatology, Eberhard Karls University, Tuebingen, Germany. [13]Werner Siemens Imaging Center, Department of Preclinical Imaging and Radiopharmacy, Eberhard Karls University, Tuebingen, Germany. [14]Cardiovascular Therapeutics, CSL Limited, Parkville, Australia. [15]Division of Infectious Diseases and Immunology, University of Massachusetts Medical School, Worcester, Massachusetts, USA. [16]German Center for Neurodegenerative Diseases, Bonn, Germany. [17]These authors contributed equally to this work. Correspondence should be addressed to E.L. (eicke.latz@uni-bonn.de).

Received 26 September; accepted 7 November; published online 8 December 2013; doi:10.1038/ni.2784

migration along a gradient of CCL2 (monocyte chemotactic protein-1; MCP-1)[17]. However, the molecular mechanisms by which HDL mediates its anti-inflammatory functions, especially in macrophages and outside of the context of atherosclerosis, remain poorly understood.

We therefore investigated the effects of HDL on activation of macrophages by TLRs and in macrophage-dependent models of inflammation under normocholesterolemic conditions. Here we show that HDL inhibits TLR-induced production of proinflammatory cytokines from macrophages. These effects were independent of HDL binding TLR ligands and did not involve modulation of TLR signaling events or disruption of cytokine secretory processes. Rather, in a time-dependent manner, HDL suppressed the ability of TLRs to induce the expression of proinflammatory cytokines (such as IL-6, IL-12p40 and TNF) on the transcriptional level. Using a systems biology approach, we identified ATF3 as an HDL-inducible negative regulator of macrophage activation. Transcriptome analysis revealed that HDL regulated many genes in an ATF3-dependent manner, and ATF3 chromatin immunoprecipitation followed by high-throughput sequencing (ChIP–seq) confirmed that several key proinflammatory genes were directly targeted by ATF3 after its induction by HDL. Furthermore, the ability of HDL to reduce TLR responses was fully dependent on expression of ATF3 both *in vitro* and *in vivo*, demonstrating the critical role of this transcriptional modulator in the anti-inflammatory effects of HDL.

## RESULTS

### HDL is protective against TLR-induced inflammation

HDL has multiple functions beyond promoting the efflux of cholesterol from lipid-laden cells. To study the anti-inflammatory effects of HDL under normocholesterolemic conditions, we used a well-established *in vivo* model of acute inflammation, in which the systemic release of proinflammatory cytokines from TLR-activated macrophages leads to liver damage[18,19]. We injected mice with HDL freshly isolated from patients ('native HDL') or with purified human apolipoprotein A1 (ApoAI; the major protein component of HDL) reconstituted with phospholipids (referred to hereafter as 'HDL') and subsequently challenged the mice with TLR agonists. Pretreatment with either native HDL or HDL significantly reduced liver damage induced by the TLR9 activator CpG DNA, as measured by release of alanine aminotransferase (ALT) or hepatocyte cell death (**Fig. 1a–c** and data not shown). In addition, mice injected with CpG after pretreatment with native HDL displayed significantly reduced serum levels of the proinflammatory cytokines IL-6 and IL-12p40 (**Fig. 1a**). Similarly, mice pretreated with HDL showed reduced serum concentrations of CpG-induced IL-6, IL-12p40, TNF, MCP-1 and IL-10 (**Fig. 1b**), whereas IL-18 and IL-13 remained unaffected (**Supplementary Fig. 1a**). In addition, HDL pretreatment significantly reduced liver damage and inflammation mediated by the TLR1 and TLR2 ligand, synthetic lipopeptide $Pam_3CSK_4$ (**Fig. 1d**). We further investigated the anti-inflammatory effect of HDL *in vitro* using bone marrow–derived macrophages (BMDMs). Pretreatment of BMDMs with HDL substantially reduced IL-6 and TNF cytokine output in response to a variety of TLR ligands (**Fig. 1e**), without impacting cell viability (**Fig. 1f**). HDL reduced TLR-mediated production of cytokines in a dose-dependent manner (**Supplementary Fig. 1b**). Using enzyme-linked immunosorbent assay (ELISA), we observed comparable decreases in TLR-induced production of IL-6 after pretreatment of BMDMs with native HDL (**Fig. 1g**). The capability

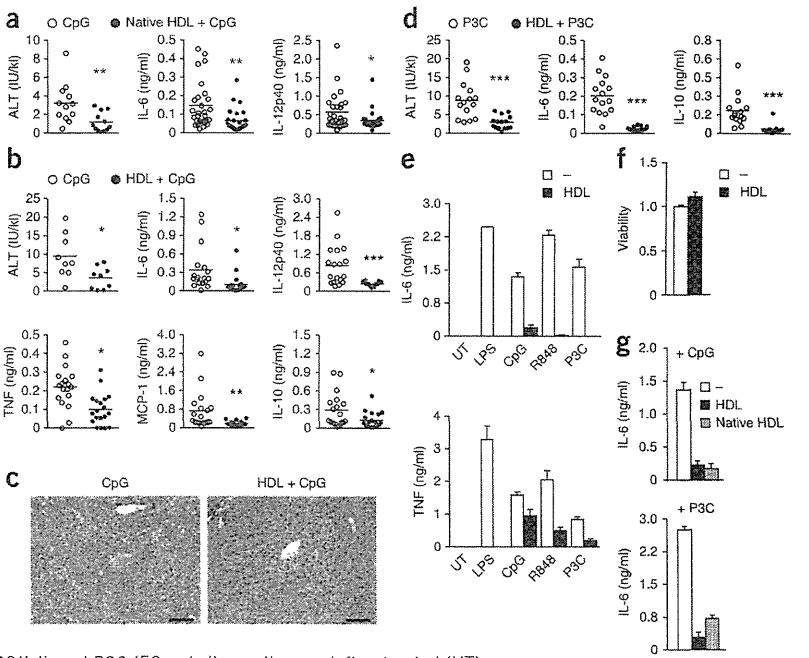


**Figure 1** HDL inhibits TLR-induced cytokine production from macrophages *in vivo* and *in vitro*. (**a–d**) Serum cytokines and ALT amounts (international units/kiloliter) measured 1 h and 10 h, respectively, after mice were injected intraperitoneally (i.p.) with 2 mg HDL for 6 h before injection of TLR ligand (i.p.; 20 μg CpG or 2 μg $Pam_3CSK_4$ (P3C)) and 10 mg D-galactosamine. In **a**, C3H/HeJ mice were injected with native HDL and CpG: ALT release ($n = 12$ mice per group) and serum cytokines (CpG, $n = 28$ mice per group; native HDL + CpG, $n = 27$ mice per group) were measured. In **b,c** C57BL/6 mice were injected with HDL and CpG; ALT release ($n = 9$ mice per group) and serum cytokines (CpG, $n = 18$ mice per group; HDL + CpG, $n = 19$ mice per group) were measured (**b**), and liver histology was assayed by hemotoxylin and eosin staining 10 h after injection (**c**; scale bars, 100 μm). In **d**, C57BL/6 mice were injected with HDL and P3C: ALT release ($n = 15$ mice per group) and serum cytokines ($n = 15$ mice per group) were measured. (**e**) ELISA of IL-6, IL-12p40 and TNF secretion from BMDMs treated with 2 mg/ml HDL or medium alone (–) for 6 h followed by overnight stimulation with the TLR4 ligand LPS (100 ng/ml), TLR9 ligand CpG (100 nM), TLR7/8 ligand R848 (5 ng/ml) or TLR2/1 ligand P3C (50 ng/ml) or cells were left untreated (UT). (**f**) Cell viability of BMDMs treated overnight with 2 mg/ml HDL or medium alone (–). (**g**) ELISA of IL-6 secretion from BMDMs pretreated with medium alone (–), HDL or native HDL (2 mg/ml) for 6 h and stimulated overnight with 100 nM CpG or 50 ng/ml P3C. Data are from one experiment (**a,b,d**; each symbol represents an individual mouse; horizontal lines indicate mean values TLR ligand versus HDL + TLR ligand, unpaired two-tailed Student's *t* test; $*P < 0.05$, $**P < 0.01$, $***P < 0.005$), representative of three mice examined per treatment, with the shown images from single mice exhibiting median expression of ALT (**c**), and combined from three independent experiments (**e,f,g**; mean + s.e.m.).

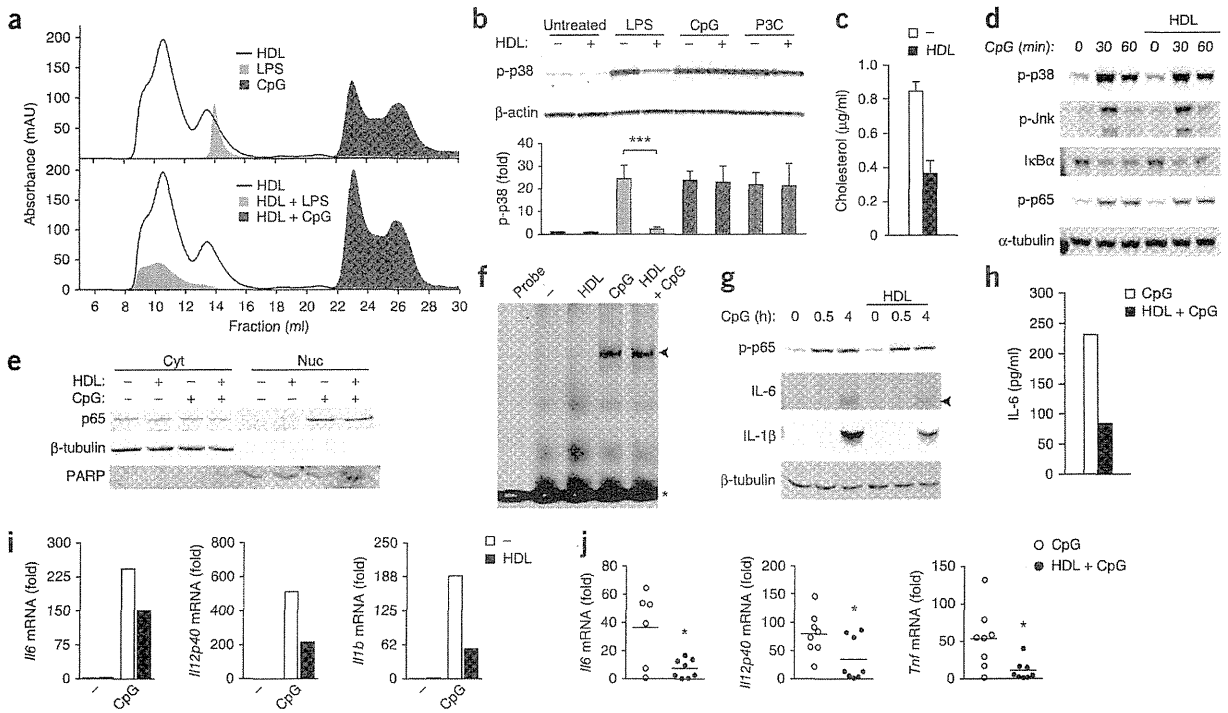


**Figure 2** HDL inhibits TLR-induced proinflammatory cytokine transcription. (**a**) Absorbance profiles of Bodipy-labeled LPS (LPS), Alexa Fluor 647–labeled CpG 1826 (CpG) and HDL, run over a Superdex-200 size-exclusion column separately (top) or together (bottom). mAU (milli absorbance units). (**b**) Immunoblot of p38 phosphorylation (p-p38) (relative to total β-actin) in whole cell lysates of untreated BMDMs or BMDMs stimulated for 30 min with 200 ng/ml LPS, 100 nM CpG or 50 ng/ml $Pam_3CSK_4$ (P3C) and incubated with 2 mg/ml HDL or medium alone (–). (**c**,**d**) Total cellular cholesterol (**c**) and immunoblots showing phosphorylation of p38 (p-p38), of Jnk (p-Jnk) and of subunit p65 of NF-κB (p-p65), and degradation of IκBα (α-tubulin was used as a loading control) in response to 100 nM CpG for indicated durations (**d**) in BMDMs pretreated with medium alone (–) or 2 mg/ml HDL for 6 h. (**e**,**f**) Immunoblots showing Subcellular localization (Cyt, cytosolic fraction; Nuc, nuclear fraction) of NF-κB p65 (β-tubulin, cytoplasmic fraction loading control; PARP, nuclear fraction loading control) (**e**) and NF-κB binding to a target probe as analyzed by electromobility shift assay (**f**) in BMDMs pretreated with 2 mg/ml HDL for 6 h before stimulation with 100 nM CpG for 30 min or left untreated (–). (**g**,**h**) CpG-induced (100 nM; indicated durations) p-p65 and intracellular IL-6 (arrow indicates IL-6 band) and IL-1β measured in whole-cell extracts (**g**) and secreted IL-6 in response to 4 h of stimulation with 100 nM CpG measured by ELISA (**h**) from BMDMs pretreated with 2 mg/ml HDL for 6 h. (**i**) mRNA expression in BMDMs pretreated with 2 mg/ml HDL for 6 h, and stimulated with 100 nM CpG for 4 h. (**j**) Liver mRNA profile 1 h after C57BL/6 mice were injected with 20 μg CpG after a 6-h pretreatment with 2 mg HDL per mouse ($n = 8$ mice per group). Data are representative of three independent experiments (**a**), representative (immunoblots) and combined (densitometic analysis) from three independent experiments (**b**, mean + s.e.m., each ligand; no HDL versus HDL incubation, unpaired two-tailed Student's $t$ test; $^{***}P < 0.005$), combined from three independent experiments (**c**, mean + s.e.m.), representative of three independent experiments (**d**–**i**), and cumulative from one experiment (**j**; each symbol represents an individual mouse and horizontal lines indicate the mean; CpG versus HDL + CpG, unpaired two-tailed Student's $t$ test; $^{*}P < 0.05$).

of HDL to decrease TLR-induced inflammation was also evident in human peripheral blood mononuclear cells (**Supplementary Fig. 1c**). Collectively, these data suggest HDL protects against TLR-induced inflammation by downmodulating the production of proinflammatory cytokines in monocytes and macrophages.

### HDL regulates inflammation at the transcriptional level

HDL can directly neutralize the inflammatory activity of the TLR4 ligand lipopolysaccharide (LPS)[20–22]. To examine whether HDL neutralizes other TLR activators by direct interaction, we analyzed whether HDL can change the size-exclusion profile of fluorescent TLR agonists. As expected, HDL led to a shift of LPS-BODIPY into the higher-molecular-weight HDL fractions (**Fig. 2a**), demonstrating binding of LPS to HDL. In contrast, HDL did not change the elution profile of CpG–Alexa Fluor 647 or $Pam_3CSK_4$–Alexa Fluor 647 (**Fig. 2a** and data not shown), indicating that HDL does not directly interact with these TLR ligands. Furthermore, direct binding by HDL should abolish or reduce the ability of TLR ligands to activate their downstream signaling pathways. Consistent with our size-exclusion data, HDL did not block CpG-induced or $Pam_3CSK_4$-induced phosphorylation of p38 MAP kinase (MAPK) (p-p38) in BMDMs, indicating successful interaction of the ligands with their receptors (**Fig. 2b**). In contrast, HDL co-treatment abolished LPS-induced p38 activation (**Fig. 2b**). These data suggest that while HDL can attenuate LPS-induced inflammation by sequestration, they do not explain the anti-inflammatory effects of HDL on other TLR ligands, including CpG and $Pam_3CSK_4$.

HDL promotes the efflux of cholesterol from macrophages and thus, subsequent TLR activation might be inhibited via changes to lipid raft cholesterol content[23,24]. However, whereas pretreatment of BMDMs with HDL decreased cellular cholesterol concentration (**Fig. 2c** and **Supplementary Fig. 2a**), it did not inhibit CpG-induced signaling, including activation of p38 MAP kinase, Jnk kinase and p65 subunit of the transcription factor NF-κB, or degradation of the inhibitory cytoplasmic NF-κB chaperone IκBα (**Fig. 2d**). Furthermore, pretreatment with HDL had no effect on the nuclear translocation of

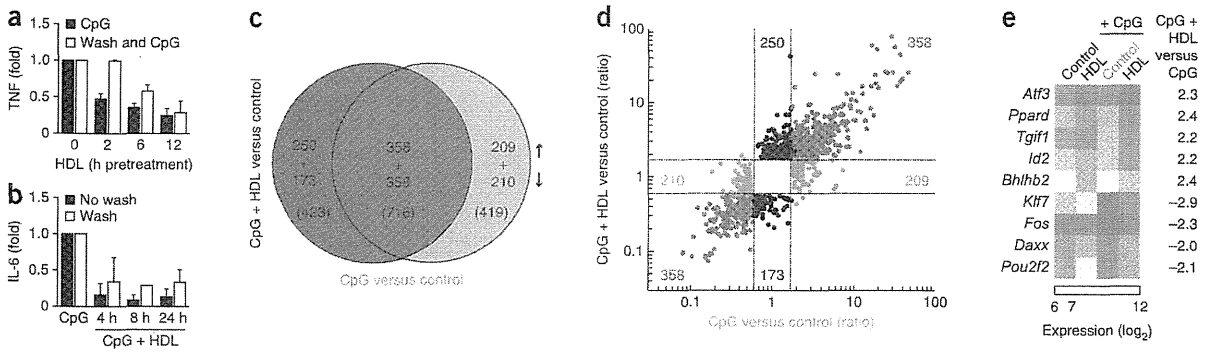


**Figure 3** Microarray analysis identifies *Atf3* as a candidate gene for the anti-inflammatory function of HDL. (**a**) TNF secretion (normalized to CpG treatment alone) from immortalized BMDMs pretreated with 2 mg/ml HDL for indicated durations, then either washed twice in serum-free DMEM, or left unwashed, before overnight stimulation with 100 nM CpG. (**b**) IL-6 secretion (normalized to CpG treatment alone) from BMDMs pretreated with 2 mg/ml HDL for 12 h, then either washed twice in serum-free DMEM, or left unwashed, before stimulation with 100 nM CpG for indicated durations. (**c–e**) Genes with differential expression (CpG or CpG + HDL versus control) and the overlap in these genes (**c**), directional gene expression resulting from CpG treatment (red), CpG + HDL treatment (blue) or genes that are coregulated in both treatments (purple) (**d**) and the most highly regulated transcription factors following HDL, CpG or CpG + HDL treatment (**e**) identified from microarray analysis of BMDMs pretreated for 6 h with 2 mg/ml HDL and then stimulated with 100 nM CpG for 4 h. Data are combined from two independent experiments (**a**,**b**; mean ± s.d.). At least three biological replicates (BMDMs from three individual mice) per condition were generated and pooled for a single microarray experiment (**c**,**d**; fold change limit 1.8, FDR-corrected $P < 0.05$, two-way ANOVA model, **e**; transcription factors are ranked according to change in expression across treatments. Color bar indicates mean expression ($log_2$) value per condition. Numbers on the right in **e** indicate the fold change of genes between CpG versus CpG + HDL.

NF-κB (**Fig. 2e**) nor did it prevent binding of NF-κB to target DNA sequences (**Fig. 2f**). Together these data exclude the possibility of interference with early TLR signaling mechanisms. To assess whether HDL affects secretion of cytokines, we measured cytokines in intracellular compartments. Although pretreatment with HDL had no effect on the activation of the p65 subunit of NF-κB in response to stimulation of TLRs, intracellular cytokine expression was diminished in BMDMs pretreated with HDL (**Fig. 2g**), as was the amount of secreted cytokines (**Fig. 2h** and **Supplementary Fig. 2b,c**). These data suggest that HDL interferes with production but not secretion of cytokines. Consistent with this hypothesis, relative expression of mRNA encoding proinflammatory cytokines was notably reduced when we treated BMDMs with HDL or native HDL before stimulation with CpG (**Fig. 2i** and **Supplementary Fig. 2d**). Cytokine mRNA expression was also decreased in the livers of mice injected with HDL or native HDL before stimulation with CpG (**Fig. 2j** and **Supplementary Fig. 2e**). We next assessed whether HDL affects the half-life of TLR-induced cytokine mRNA or protein. Pretreatment of BMDMs with HDL did not alter the stability of *Il6* mRNA (**Supplementary Fig. 2f**) nor the stability of IL-1β protein (**Supplementary Fig. 2g**). Together these data indicate that HDL may regulate anti-inflammatory effects in macrophages, by downmodulating transcription of proinflammatory genes.

### ATF3 is identified as a candidate transcription factor

We noted that macrophages exposed to HDL for longer periods of time displayed a more pronounced reduction in the production of cytokines (**Fig. 3a**), which persisted up to 24 h after removal of HDL (**Fig. 3b**). This suggested that the underlying molecular mechanism might involve *de novo* transcription of an inflammatory repressor. We therefore used genome-wide RNA profiling to assess whether HDL affected the transcriptional response to TLR stimulation, by comparing resting BMDMs with HDL-pretreated BMDMs that we subsequently stimulated with CpG. Principle component analysis and hierarchical clustering indicated that HDL induced profound transcriptional changes in resting and CpG-treated BMDMs (**Supplementary Fig. 3a,b**). As expected, treatment with HDL alone induced the gene expression of several enzymes involved in the cholesterol biosynthesis pathway (**Supplementary Fig. 3c**). This finding correlated with an increased appearance of cholesterol precursors after treatment with HDL, as identified by mass spectrometry analysis (**Supplementary Fig. 3d**). Stimulation of BMDMs with CpG resulted in regulation of 1,135 genes in total, 419 of which were not influenced by pretreatment with HDL (**Fig. 3c,d**). The remaining 716 CpG-regulated genes (**Fig. 3c**) were also regulated by CpG in the presence of HDL relative to resting cells. However, HDL further enhanced or reduced the expression of many of these genes (**Fig. 3d**). HDL treatment also modulated the expression of 423 genes (250 induced and 173 repressed) independently of CpG treatment (**Fig. 3c,d**). To identify a potential transcription factor that might be responsible for the anti-inflammatory effects of HDL, we interrogated our transcriptome data using several bioinformatics approaches. First, we performed Gene Ontology enrichment analysis (GOEA) using the genes that were regulated by CpG and further modified by HDL and visualized this as a GO term network (**Supplementary Fig. 3e**). This analysis identified one subnet, based on genes downregulated by HDL, that could be summarized as 'innate immune response'-related processes, and another large subnet, based on genes induced by HDL, that was linked to cholesterol and lipid metabolism. However, a group of GO terms with the highest enrichment scores were linked to a central dense subnet best summarized as 'regulation of metabolic processes'. Based on this pronounced enrichment of regulatory processes we searched for candidates of transcriptional regulation in this subnet and identified the transcriptional regulator ATF3 in most of the subnet's GO terms (**Supplementary Fig. 3e**). Second, using the transcription factor (TF) catalog database (TFCat database)[25], we identified ATF3 as the TF with the highest expression in the presence of HDL (**Fig. 3e**). Finally, we performed TF promoter-binding prediction using the genes most significantly repressed by HDL as bait (fold change < −3, false discovery rate (FDR)-corrected $P < 0.05$, two-way analysis of variance (ANOVA), $n = 33$ genes; (Online Methods and **Supplementary Fig. 3f**). Among the 143 TF candidates potentially binding to these promoters, only ATF3 (fold change, 2.3) was upregulated by HDL. TF module analysis validated these findings and identified potential ATF3 binding

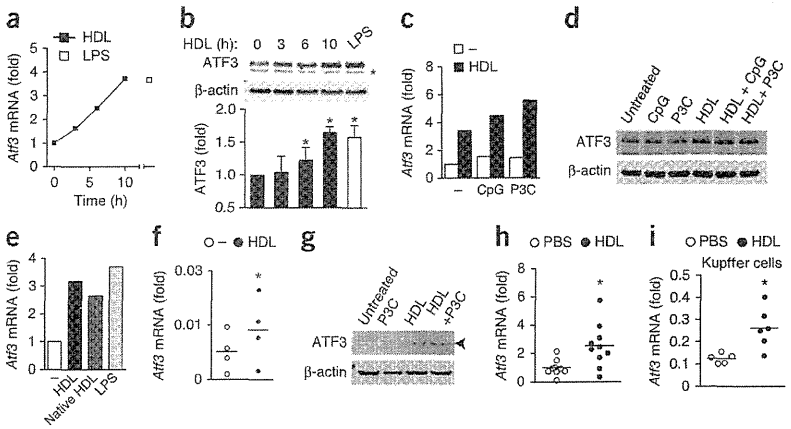


**Figure 4** HDL induces ATF3 expression. (**a**,**b**) Amounts of *Atf3* mRNA (**a**) or ATF3 protein (**b**; relative to total β-actin; * indicates a nonspecific band) from BMDMs treated with 2 mg/ml HDL for the indicated durations or 200 ng/ml LPS for 6 h. (**c**,**d**) Amounts of *Atf3* mRNA (**c**) and ATF3 protein (**d**) from BMDMs pretreated with 2 mg/ml HDL or medium alone (–) for 6 h and stimulated with 100 nM CpG or 50 ng/ml $Pam_3CSK_4$ (P3C) for 4 h, or left untreated. (**e**) *Atf3* mRNA expression in BMDMs treated with medium alone (–), 2 mg/ml HDL, 2 mg/ml native HDL or 200 ng/ml LPS for 10 h. (**f**,**g**) Amounts of *Atf3* mRNA (**f**) or ATF3 protein (**g**; arrow indicates ATF3 band) from $CD14^+$ monocytes pretreated with medium alone (–) or 2 mg/ml HDL for 6 h, and stimulated with 1 μg/ml P3C for 4 h. (**h**,**i**) Amounts of *Atf3* mRNA from livers ($n = 9$ mice per group; **h**) or Kupffer cells ($n = 6$ mice per group; **i**) of C57BL/6 mice 10 h after intraperitoneal injection of 2 mg HDL. Data are representative of three independent experiments (**a**,**c**,**e**), representative of four independent experiments (**b**; mean + s.e.m.; untreated versus HDL-treated, unpaired two-tailed Student's *t* test, $^*P < 0.05$), representative of at least two independent experiments (**d**,**g**), and from single experiments (**f**,**h**,**i**; individual symbols represent an individual donors and horizontal lines indicate mean; in **f**: untreated versus HDL-treated, paired one-tailed Student's *t* test, $^*P < 0.05$ and in **h**,**i**: PBS versus HDL-injected mice, unpaired two-tailed Student's *t* test; $^*P < 0.05$).



sites in 28 of 33 input genes (Online Methods and **Supplementary Table 1**). Collectively, these analyses strongly support a model in which HDL leads to the repression of CpG-induced genes by increasing the expression of the transcriptional regulator ATF3.

### ATF3 binds target gene promoters after HDL induction

Consistent with our transcriptome analysis, BMDMs treated with HDL displayed increased expression of *Atf3* mRNA and ATF3 protein in a time-dependent manner (**Fig. 4a**,**b**). The induction of *Atf3* mRNA and ATF3 protein by HDL was further potentiated by subsequent stimulation with CpG or $Pam_3CSK_4$ (**Fig. 4c**,**d**). Native HDL also induced *Atf3* mRNA expression to comparable levels in BMDMs (**Fig. 4e**). Additionally, treatment with HDL increased amounts of *ATF3* mRNA and ATF3 protein in human monocytes (**Fig. 4f**,**g**). *In vivo*, HDL injection increased hepatic *Atf3* mRNA expression in C57BL/6 mice (**Fig. 4h**), specifically in Kupffer cells (the resident macrophages of the liver; **Fig. 4i**). To analyze whether HDL treatment would modulate ATF3 binding to target gene promoters, we performed ATF3 ChIP-seq on wild-type and *Atf3*-deficient BMDMs. We used signals from *Atf3*-deficient BMDMs to subtract background nonspecific binding of the ATF3 antibody. HDL treatment, either alone or in combination with CpG treatment, dramatically increased ATF3 binding across the genome, whereas CpG treatment alone reduced ATF3 binding (**Fig. 5a**). Global assessment of ATF3 peak localization relative to transcription start sites revealed that ATF3 was specifically enriched at promoter regions of genes (**Fig. 5b**). Consistent with our findings that HDL treatment resulted in reduced production of proinflammatory cytokines, our ChIP-seq analysis demonstrated specific ATF3 binding at the promoters of genes encoding IL-6, IL-12p40 and TNF in the presence of HDL or HDL plus CpG, but not CpG alone (**Fig. 5c**). We observed no enrichment of ATF3 at promoters of the non–HDL-regulated cytokines that we identified *in vivo* (**Supplementary Fig. 1a**) such as IL-18 and IL-13 (**Supplementary Fig. 4a**). Together these data demonstrate that after induction by HDL, ATF3 is specifically enriched at the promoters of cytokines found to be regulated by HDL both *in vivo* and *in vitro*, strongly suggesting that the anti-inflammatory effects of HDL are mediated via this mechanism.

Functions of HDL are most intimately associated with processes related to atherosclerosis. Thus, we next examined whether ATF3 was induced after HDL treatment in an animal model of atherosclerosis. We examined the livers of atherosclerosis-prone *Apoe*-deficient mice fed a high-fat diet and observed that HDL-injected mice displayed significantly greater hepatic *Atf3* mRNA expression compared with PBS-injected control mice (**Fig. 5d**). Induction of ATF3 correlated with a substantial reduction in the levels of the direct ATF3 target genes encoding IL-6, IL-12p40 and cholesterol 25-hydroxylase (Ch25h) (**Fig. 5e**). Notably, in the livers of HDL-injected *Apoe*-deficient mice, we observed a significant ($P = 0.0092$, unpaired two-tailed Student's *t* test) induction of *Atf3* mRNA in Kupffer cells, whereas hepatocytes showed tenfold less expression (**Supplementary Fig. 4b**). These data demonstrate that in an animal model of atherosclerosis, HDL induces the expression of ATF3 in macrophages, which may repress expression of inflammatory target genes.

### HDL's anti-inflammatory effects are mediated via ATF3

To further assess the role of ATF3 in mediating the anti-inflammatory effects of HDL, we performed genome-wide transcriptome analysis on wild-type and *Atf3*-deficient BMDMs pretreated with HDL and subsequently stimulated with CpG or $Pam_3CSK_4$. Using the model presented in **Figure 6a**, we observed that ATF3 deficiency affected a large set of TLR-driven, HDL-modulated genes (224 probes detecting 188 genes; **Supplementary Table 2a**). Transcripts induced or repressed in wild-type BMDMs by CpG or $Pam_3CSK_4$ alone and counter-regulated by pretreatment with HDL were no longer modified in the absence of ATF3 (**Fig. 6b**, **Supplementary Fig. 5a** and **Supplementary Table 2b–e**). We observed substantially overlapping gene sets when CpG or $Pam_3CSK_4$ stimulation was used (**Supplementary Fig. 5b**). Furthermore, GOEA network visualization of TLR-regulated genes demonstrated that immune response–related functions modified by HDL were ATF3-dependent, whereas lipid metabolism terms were ATF3-independent (**Supplementary Fig. 5c**). In fact, the majority of genes in the cholesterol biosynthesis pathway showed ATF3-independent regulation by HDL (**Supplementary Fig. 5d**). Accordingly, we did not detect differential gene expression between wild-type and *Atf3*-deficient BMDMs for *Srebf2* (ref. 26) or *Nr1h3* (gene encoding LXR) target genes[27] (data not shown), indicating that ATF3 is not involved in their regulation in response to HDL. Of the genes we identified to be regulated by HDL and CpG in wild-type cells but not in *Atf3*-deficient cells

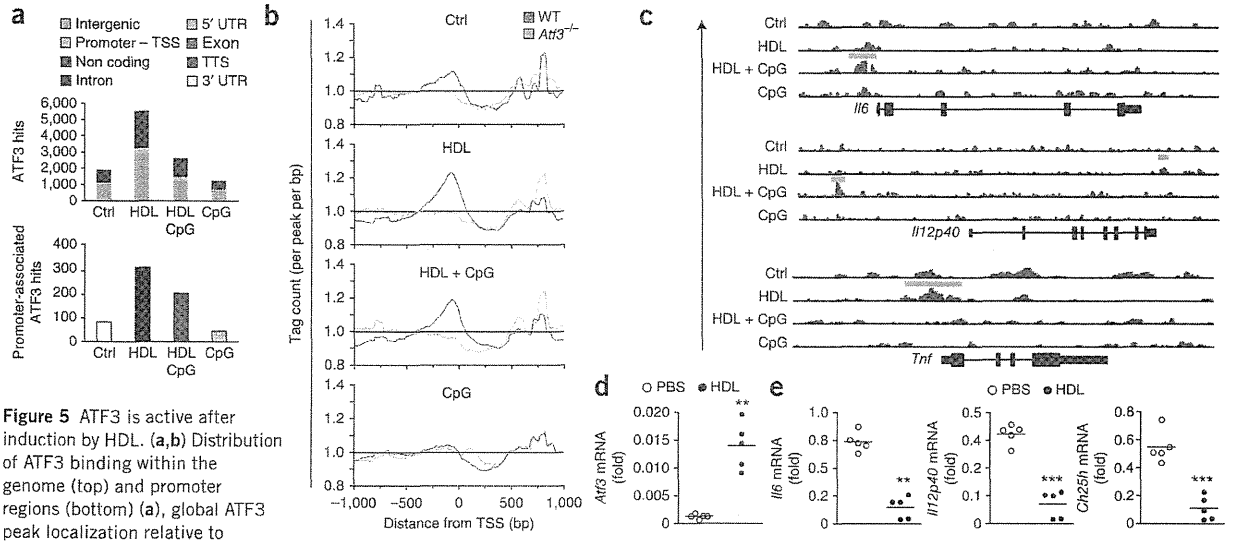


**Figure 5** ATF3 is active after induction by HDL. (**a**,**b**) Distribution of ATF3 binding within the genome (top) and promoter regions (bottom) (**a**), global ATF3 peak localization relative to transcription start site (TSS) (**b**; normalized average of tags per peak per base pair from −1 kb to +1 kb) and genomic loci of *Il6*, *Il12p40* and *Tnf* with ChIP-seq signals for ATF3 binding (**c**; red bars indicate significant peaks; $P < 10^{-5}$, FDR < 0.1; Online Methods) from ATF3 ChIP-seq for BMDMs pretreated with medium alone (ctrl) or 2 mg/ml HDL for 6 h followed by stimulation with 100 nM CpG for 4 h. UTR, untranslated region. TTS, transcription termination site. (**d**,**e**) mRNA from livers of *Apoe*-deficient mice fed on a high-fat diet and injected intravenously (i.v.) with PBS or 100 mg/kg HDL ($n = 5$ mice per group). At least three biological replicates (BMDMs from three individual mice) per condition were generated and pooled for a single ChIP-seq experiment (**a**–**c**). Data are pooled from single experiments (**d**,**e**; symbols represent individual mice and horizontal lines indicate the mean; PBS versus HDL-treated, unpaired two-tailed Student's *t* test, $^{**}P < 0.01$, $^{***}P < 0.001$).



($n = 130$ genes), ~20% were confirmed as direct ATF3 target genes ($n = 27$ genes) by ChIP-seq, and analysis of GO terms of these direct ATF3 targets identified specific enrichment of genes involved in inflammatory processes (**Supplementary Fig. 5e**).

To confirm that ATF3 was required for HDL-mediated inhibition of TLR-induced cytokine secretion, we compared the effects of pretreatment with HDL on subsequent TLR responses in wild-type and *Atf3*-deficient BMDMs. As expected, HDL significantly reduced CpG-induced production of IL-6 and IL-12p40 in wild-type BMDMs but not in *Atf3*-deficient BMDMs (**Fig. 7a**). Additionally, we assessed the relevance of ATF3 induction by HDL *in vivo* by comparing wild-type and *Atf3*-deficient mice subjected to inflammation and liver injury induced by injection of CpG. HDL was no longer protective against CpG-induced liver damage in *Atf3*-deficient mice, as observed by comparable amounts of ALT release from *Atf3*-deficient mice injected with or without HDL (**Fig. 7b**). Accordingly, unlike wild-type mice, *Atf3*-deficient mice injected with HDL showed no significant reductions in serum concentration of IL-12p40 and TNF or in hepatic TNF protein expression in response to CpG (**Fig. 7b**). These data demonstrate that repression of proinflammatory cytokine responses by HDL both *in vitro* and *in vivo* is mediated by the induction of ATF3.

The protective functions of HDL are best documented in the context of atherosclerosis. Cardiovascular risk factors including hypertension, toxins from cigarette smoke, high blood sugar and turbulent blood flow can lead to localized and recurrent endothelial damage, a process thought to be critical in atherogenesis[28]. Endothelial damage is followed by an inflammatory response of macrophages that modulates the rate and extent of re-endothelialization[29,30]. As HDL is known to accelerate vascular wound healing and re-endothelialization[31–33], we next assessed whether ATF3 is also critical for the protective function of HDL in an atherosclerosis-relevant model of vascular repair. Whereas HDL effectively increased the amount of re-endothelialization after carotid artery injury in wild-type mice, we observed no change in *Atf3*-deficient mice (**Fig. 7c,d**). These data suggest that HDL can dampen the local inflammation that occurs during vascular injury and that ATF3 thereby contributes to the vascular repair process. To broadly assess the effects of HDL in the vascular wall after injury, we performed transcriptional profiling of RNA isolated from the injured carotid artery segments from wild-type and *Atf3*-deficient mice that were injected with HDL or PBS. Hierarchical clustering of genes and samples showed that the replicate samples in the four groups clustered as four individual groups (**Supplementary Fig. 6a**). HDL treatment strongly modulated genes in wild-type samples but not in *Atf3*-deficient samples, implying that the effects of HDL treatment

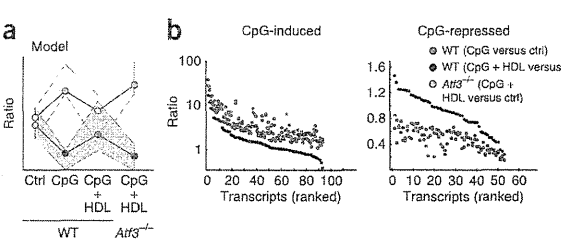


**Figure 6** ATF3 mediates much of the transcriptional response to HDL treatment of macrophages. (**a**,**b**) The model used to identify ATF3-dependent HDL target genes (**a**) and transcripts induced (left) or repressed (right) by CpG versus control (ctrl) (green dots) and counter-regulated by HDL treatment (black dots) in wild-type (WT) BMDMs and no longer counter-regulated by HDL in *Atf3*-deficient BMDMs (red dots) (**b**) from microarray analysis of WT and *Atf3*-deficient BMDMs pretreated with medium alone (ctrl) or 2 mg/ml HDL for 6 h and subsequently stimulated for 4 h with 100 nM CpG. At least three biological replicates (BMDMs from three individual mice) per condition were generated and pooled for a single microarray experiment. In **a**, red and blue shading indicates genes 'increased' and repressed by CpG treatment, respectively. Colored dots represent individual transcripts in **b**.

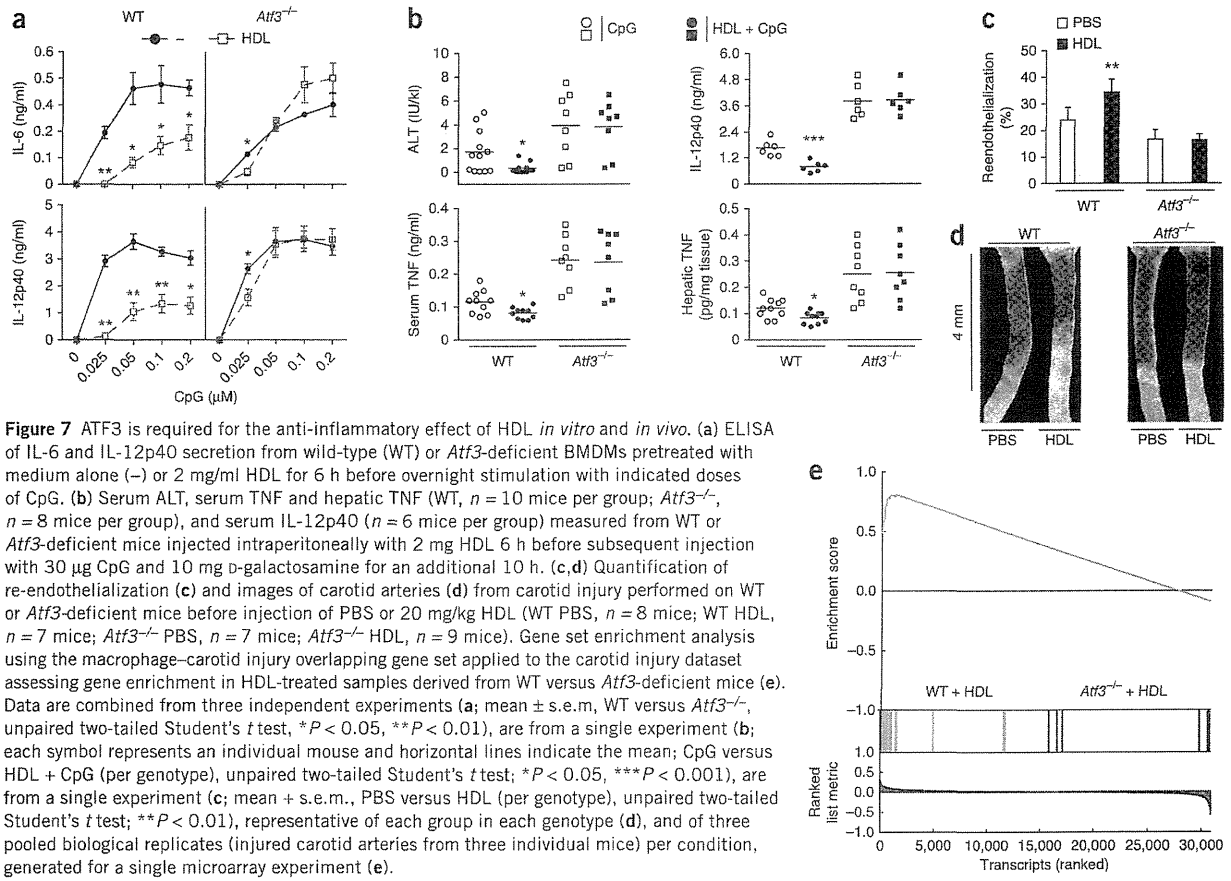


**Figure 7** ATF3 is required for the anti-inflammatory effect of HDL *in vitro* and *in vivo*. (**a**) ELISA of IL-6 and IL-12p40 secretion from wild-type (WT) or *Atf3*-deficient BMDMs pretreated with medium alone (–) or 2 mg/ml HDL for 6 h before overnight stimulation with indicated doses of CpG. (**b**) Serum ALT, serum TNF and hepatic TNF (WT, $n = 10$ mice per group; $Atf3^{-/-}$, $n = 8$ mice per group), and serum IL-12p40 ($n = 6$ mice per group) measured from WT or *Atf3*-deficient mice injected intraperitoneally with 2 mg HDL 6 h before subsequent injection with 30 μg CpG and 10 mg D-galactosamine for an additional 10 h. (**c**,**d**) Quantification of re-endothelialization (**c**) and images of carotid arteries (**d**) from carotid injury performed on WT or *Atf3*-deficient mice before injection of PBS or 20 mg/kg HDL (WT PBS, $n = 8$ mice; WT HDL, $n = 7$ mice; $Atf3^{-/-}$ PBS, $n = 7$ mice; $Atf3^{-/-}$ HDL, $n = 9$ mice). Gene set enrichment analysis using the macrophage–carotid injury overlapping gene set applied to the carotid injury dataset assessing gene enrichment in HDL-treated samples derived from WT versus *Atf3*-deficient mice (**e**). Data are combined from three independent experiments (**a**; mean ± s.e.m, WT versus $Atf3^{-/-}$, unpaired two-tailed Student's *t* test, $^{*}P < 0.05$, $^{**}P < 0.01$), are from a single experiment (**b**; each symbol represents an individual mouse and horizontal lines indicate the mean; CpG versus HDL + CpG (per genotype), unpaired two-tailed Student's *t* test; $^{*}P < 0.05$, $^{***}P < 0.001$), are from a single experiment (**c**; mean + s.e.m., PBS versus HDL (per genotype), unpaired two-tailed Student's *t* test; $^{**}P < 0.01$), representative of each group in each genotype (**d**), and of three pooled biological replicates (injured carotid arteries from three individual mice) per condition, generated for a single microarray experiment (**e**).

were dependent on the presence of ATF3 (**Supplementary Fig. 6a**). We next characterized the genes regulated by HDL and ATF3 in carotid artery samples and overlapped them with those genes earlier identified as regulated by HDL via ATF3 in macrophages *in vitro* (**Fig. 6** and **Supplementary Fig. 5**). We performed GOEA analysis with these genes and visualized the changes of GO terms resulting from treatment with HDL in wild-type but not ATF3-deficient samples using Biological Networks Gene Ontology tool (BINGO). Consistent with our *in vitro* macrophage analysis, treatment with HDL led to an ATF3-dependent reduction of the inflammatory responses in carotid artery samples (**Supplementary Fig. 6b**). We validated these approaches using gene set enrichment analysis (GSEA) on the macrophage–carotid injury overlapping gene set. GSEA ranks RNA expression results based on their correlation with the phenotype and significant (FDR < 0.001, $P < 0.001$, empirical phenotype-based permutation test procedure) enrichment. These analyses revealed a highly significant enrichment of these ATF3 target gene sets in HDL-treated samples from wild-type mice but not *Atf3*-deficient mice (**Fig. 7e**). These data indicate that the beneficial effects of HDL on carotid artery re-endothelialization are for the most part driven by ATF3 and the reduction of macrophage inflammation.

## DISCUSSION

Epidemiological studies have consistently documented that low concentrations of HDL cholesterol in the blood represent a strong, independent risk factor for cardiovascular disease. The protective effect of HDL in cardiovascular and possibly other inflammatory diseases is thought to be the result of several beneficial functions. HDL relieves cells from excessive amounts of cholesterol, has strong antioxidative effects, inhibits platelet aggregation and exerts several vasoprotective effects[34]. Most notably, HDL also has the remarkable ability to modulate the inflammatory response in various cell types. HDL isolated from healthy individuals or reconstituted from purified ApoA1 and phospholipids is strongly anti-inflammatory. However, during an acute phase response or in chronic inflammatory states, HDL can be modified to become dysfunctional[33].

The mechanisms by which HDL reduces inflammatory responses, particularly in macrophages, are not well understood. Although it is known that HDL can sequester LPS and thereby prevent cellular activation through TLR4, this mechanism does not explain why HDL can block a broad spectrum of TLR-mediated inflammatory responses in macrophages. In contrast to the current understanding that HDL can impair TLR signaling by interfering with amounts of raft cholesterol, we found that TLR signaling and subsequent nuclear translocation of the proinflammatory transcription factor NF-κB remained unaffected by HDL. We identified that the induction of ATF3, a key transcriptional modulator of innate immune response genes, is the main mechanism by which HDL mediates its anti-inflammatory activities in macrophages. ATF3 can be induced by TLR activation and acts as part of an important negative-feedback loop to limit TLR-driven inflammatory responses in macrophages. Hence, by inducing ATF3, HDL uses an ancient regulatory feedback system and can broadly and directly modify the inflammatory response of macrophages toward TLR stimulation.

This discovery has broad implications as TLR activation triggers macrophage responses that contribute to a large number of inflammatory pathologies. For example, targeted deletion of TLRs or components of their signaling pathways in mice confers protection against atherosclerosis[35–37]. Furthermore, TLR-inducible proinflammatory cytokines such as IL-6, IL-12p40 and TNF all contribute to development of atherosclerosis[38]. Of note, ATF3 can also directly regulate cholesterol metabolism pathways by repressing expression of Ch25h, an enzyme required for 25-hydroxycholesterol–mediated formation of foam cells. Indeed, mice deficient in both ATF3 and ApoE have enhanced atherosclerotic lesions, which has been attributed to increased expression of Ch25h (ref. 39). Consistently, we observed that injection of HDL in *Apoe*-deficient mice induced ATF3 expression and reduced the expression of Ch25h as well as of the proinflammatory cytokines IL-6 and IL-12p40. Hence, HDL appears to modulate both foam-cell formation and inflammation via ATF3, which could contribute to HDL's protective nature in atherosclerosis. However, HDL is known to exert other effects that can beneficially influence atherosclerosis that are likely independent of ATF3. For example, HDL's antioxidative function can prevent oxidation of LDL, which itself contributes to atherogenesis[17]. Modulation of cellular cholesterol by HDL may also affect antigen presentation and the induction of an adaptive immune response[16]. Furthermore, HDL reverses hyperproliferation of hematopoietic stem cell precursors, which can exaggerate atherosclerosis[40]. Similarly, HDL affects the activation of platelets, which do not have a nucleus[41], and it reduces the integrin-mediated adhesion of leukocytes too quickly to involve transcription[42]. Therefore, the contribution of ATF3 to HDL's protective effects against atherosclerosis *in vivo* may be difficult to separate from the rest of its protective functions.

Our ChIP-seq analysis in macrophages, and RNA profiling studies in macrophages and injured carotid arteries revealed that HDL regulates an exceptionally broad set of target genes via ATF3 under normocholesterolemic conditions. This could be explained by the ability of ATF3 to recruit corepressors such as histone deacetylase 1 (HDAC1). Recruitment of HDAC1 by ATF3 is thought to result in less histone acetylation at target gene promoters, which is typically associated with a closed chromatin and inactivation of genes[3,39]. Thus, via this mechanism, HDL could influence epigenetic modification of target genes. Indeed, we observed that ATF3 was constitutively bound across target gene promoters in resting macrophages, which was lost upon stimulation with CpG, consistent with transcriptional activation of these genes. However, HDL treatment further increased ATF3 binding across the genome, presumably remodeling chromatin structure to prevent transcriptional activation of these genes. These results provide a long-sought mechanistic link between HDL and its anti-inflammatory function.

Although the protective role of HDL is most well characterized in atherosclerosis, the capability of HDL to broadly modulate TLR responses suggests that HDL may be beneficial in other chronic inflammatory diseases. Our findings raise the possibility of using HDL-based therapeutics in treating inflammatory disorders not directly linked to hypercholesterolemia. Furthermore, our results imply that fine-tuning the negative regulators of inflammation, such as ATF3, may provide a therapeutic avenue for the treatment of a range of inflammatory pathologies.

## METHODS

Methods and any associated references are available in the online version of the paper.

**Accession codes.** Gene Expression Omnibus (GEO): GSE44034.

*Note: Any Supplementary Information and Source Data files are available in the online version of the paper.*

ACKNOWLEDGMENTS

We acknowledge C. Thiele (University of Bonn) for helpful discussions and J.-C. Hernandez (University of Medellin) for help with experiments. We thank C.M. De Nardo for critical reading of the manuscript. We thank T. Hai (Ohio State University) for the original *Atf3*-deficient mice. The work was funded by grants from US National Institutes of Health (1R01HL093262 to E.L., and 1R01HL112661 to E.L. and M.L.F.), the German Research foundation (SFB670 to E.L., SFB685 to M.Kn. and M.R.), the Excellence Cluster ImmunoSensation to E.L. and J.L.S., the Australian National Health and Medical Research Council (1006588), the Operational Infrastructure Support Program (Victoria state Government, Australia) to B.R.G.W. and D.X., and the Naito Foundation (Japan) and the Ministry of Health, Labour and Welfare and Grant-in-Aid for Scientific Research on Innovative Areas for Scientific Research from the Ministry of Education, Culture, Sports, Science and Technology of Japan to H.K. E.L. is a member of the Center for Molecular Inflammation Research at the Norwegian University of Science and Technology.

AUTHOR CONTRIBUTIONS

D.D., L.I.L., H.K. and R.S. designed and performed experiments and analyzed data. S.V.S., D.X., F.A.S., J.V., A.K., M.Kr., N.B., A.G., C.L., S.Z. and N.J.H. performed experiments. S.V.S., M.B., T.U., W.K. and J.L.S. analyzed transcriptome and ChIP sequencing data. M.Kn. and M.R. provided the *Atf3*-deficient and matched wild-type control mice. D.L., M.L.F., B.R.G.W., P.K. and S.D.W. analyzed data and provided critical suggestions and discussions throughout the study. D.D., L.I.L., J.L.S. and E.L. designed the study and, along with S.D.W., wrote the paper.

COMPETING FINANCIAL INTERESTS

The authors declare competing financial interests: details are available in the online version of the paper.



1. Takeuchi, O. & Akira, S. Pattern recognition receptors and inflammation. *Cell* **140**, 805–820 (2010).
2. Medzhitov, R. & Horng, T. Transcriptional control of the inflammatory response. *Nat. Rev. Immunol.* **9**, 692–703 (2009).
3. Gilchrist, M. *et al.* Systems biology approaches identify ATF3 as a negative regulator of Toll-like receptor 4. *Nature* **441**, 173–178 (2006).
4. Hai, T., Wolford, C.C. & Chang, Y.S. ATF3, a hub of the cellular adaptive-response network, in the pathogenesis of diseases: is modulation of inflammation a unifying component? *Gene Expr.* **15**, 1–11 (2010).
5. Whitmore, M.M. *et al.* Negative regulation of TLR-signaling pathways by activating transcription factor-3. *J. Immunol.* **179**, 3622–3630 (2007).
6. Duewell, P. *et al.* NLRP3 inflammasomes are required for atherogenesis and activated by cholesterol crystals. *Nature* **464**, 1357–1361 (2010).
7. Seneviratne, A.N., Sivagurunathan, B. & Monaco, C. Toll-like receptors and macrophage activation in atherosclerosis. *Clin. Chim. Acta* **413**, 3–14 (2012).
8. Gordon, T., Castelli, W.P., Hjortland, M.C., Kannel, W.B. & Dawber, T.R. High density lipoprotein as a protective factor against coronary heart disease. The Framingham Study. *Am. J. Med.* **62**, 707–714 (1977).
9. Mineo, C. & Shaul, P.W. Novel biological functions of high-density lipoprotein cholesterol. *Circ. Res.* **111**, 1079–1090 (2012).
10. Schwartz, G.G. *et al.* Effects of dalcetrapib in patients with a recent acute coronary syndrome. *N. Engl. J. Med.* **367**, 2089–2099 (2012).
11. Boden, W.E. *et al.* Niacin in patients with low HDL cholesterol levels receiving intensive statin therapy. *N. Engl. J. Med.* **365**, 2255–2267 (2011).
12. Rader, D.J. & Tall, A.R. The not-so-simple HDL story: Is it time to revise the HDL cholesterol hypothesis? *Nat. Med.* **18**, 1344–1346 (2012).
13. Khera, A.V. *et al.* Cholesterol efflux capacity, high-density lipoprotein function, and atherosclerosis. *N. Engl. J. Med.* **364**, 127–135 (2011).
14. Libby, P., Ridker, P.M. & Hansson, G.K. Progress and challenges in translating the biology of atherosclerosis. *Nature* **473**, 317–325 (2011).
15. Murphy, A.J., Westerterp, M., Yvan-Charvet, L. & Tall, A.R. Anti-atherogenic mechanisms of high density lipoprotein: effects on myeloid cells. *Biochim. Biophys. Acta* **1821**, 513–521 (2012).
16. Norata, G.D., Pirillo, A., Ammirati, E. & Catapano, A.L. Emerging role of high density lipoproteins as a player in the immune system. *Atherosclerosis* **220**, 11–21 (2012).
17. Barter, P.J. *et al.* Antiinflammatory properties of HDL. *Circ. Res.* **95**, 764–772 (2004).
18. Hemmi, H. *et al.* A Toll-like receptor recognizes bacterial DNA. *Nature* **408**, 740–745 (2000).
19. Sparwasser, T. *et al.* Macrophages sense pathogens via DNA motifs: induction of tumor necrosis factor-alpha-mediated shock. *Eur. J. Immunol.* **27**, 1671–1679 (1997).

20. Ulevitch, R.J. & Johnston, A.R. The modification of biophysical and endotoxic properties of bacterial lipopolysaccharides by serum. *J. Clin. Invest.* **62**, 1313–1324 (1978).
21. Levine, D.M., Parker, T.S., Donnelly, T.M., Walsh, A. & Rubin, A.L. In vivo protection against endotoxin by plasma high density lipoprotein. *Proc. Natl. Acad. Sci. USA* **90**, 12040–12044 (1993).
22. Wurfel, M.M., Hailman, E. & Wright, S.D. Soluble CD14 acts as a shuttle in the neutralization of lipopolysaccharide (LPS) by LPS-binding protein and reconstituted high density lipoprotein. *J. Exp. Med.* **181**, 1743–1754 (1995).
23. Triantafilou, M., Miyake, K., Golenbock, D.T. & Triantafilou, K. Mediators of innate immune recognition of bacteria concentrate in lipid rafts and facilitate lipopolysaccharide-induced cell activation. *J. Cell Sci.* **115**, 2603–2611 (2002).
24. Zhu, X. *et al.* Macrophage ABCA1 reduces MyD88-dependent Toll-like receptor trafficking to lipid rafts by reduction of lipid raft cholesterol. *J. Lipid Res.* **51**, 3196–3206 (2010).
25. Fulton, D.L. *et al.* TFCat: the curated catalog of mouse and human transcription factors. *Genome Biol.* **10**, R29 (2009).
26. Horton, J.D. *et al.* Combined analysis of oligonucleotide microarray data from transgenic and knockout mice identifies direct SREBP target genes. *Proc. Natl. Acad. Sci. USA* **100**, 12027–12032 (2003).
27. Heinz, S. *et al.* Simple combinations of lineage-determining transcription factors prime cis-regulatory elements required for macrophage and B cell identities. *Mol. Cell* **38**, 576–589 (2010).
28. Zimarino, M. *et al.* Optical coherence tomography accurately identifies intermediate atherosclerotic lesions—an *in vivo* evaluation in the rabbit carotid artery. *Atherosclerosis* **193**, 94–101 (2007).
29. Carmeliet, P. *et al.* Vascular wound healing and neointima formation induced by perivascular electric injury in mice. *Am. J. Pathol.* **150**, 761–776 (1997).
30. Zimmer, S. *et al.* Activation of endothelial toll-like receptor 3 impairs endothelial function. *Circ. Res.* **108**, 1358–1366 (2011).
31. Seetharam, D. *et al.* High-density lipoprotein promotes endothelial cell migration and reendothelialization via scavenger receptor-B type I. *Circ. Res.* **98**, 63–72 (2006).
32. Petoumenos, V., Nickenig, G. & Werner, N. High-density lipoprotein exerts vasculoprotection via endothelial progenitor cells. *J. Cell Mol. Med.* **13**, 4623–4635 (2009).
33. Speer, T. *et al.* Abnormal high-density lipoprotein induces endothelial dysfunction via activation of Toll-like receptor-2. *Immunity* **38**, 754–768 (2013).
34. Saemann, M.D. *et al.* The versatility of HDL: a crucial anti-inflammatory regulator. *Eur. J. Clin. Invest.* **40**, 1131–1143 (2010).
35. Michelsen, K.S. *et al.* Lack of Toll-like receptor 4 or myeloid differentiation factor 88 reduces atherosclerosis and alters plaque phenotype in mice deficient in apolipoprotein E. *Proc. Natl. Acad. Sci. USA* **101**, 10679–10684 (2004).
36. Mullick, A.E., Tobias, P.S. & Curtiss, L.K. Modulation of atherosclerosis in mice by Toll-like receptor 2. *J. Clin. Invest.* **115**, 3149–3156 (2005).
37. Kim, T.W. *et al.* The critical role of IL-1 receptor-associated kinase 4-mediated NF-kappaB activation in modified low-density lipoprotein-induced inflammatory gene expression and atherosclerosis. *J. Immunol.* **186**, 2871–2880 (2011).
38. Kleemann, R., Zadelaar, S. & Kooistra, T. Cytokines and atherosclerosis: a comprehensive review of studies in mice. *Cardiovasc. Res.* **79**, 360–376 (2008).
39. Gold, E.S. *et al.* ATF3 protects against atherosclerosis by suppressing 25-hydroxycholesterol-induced lipid body formation. *J. Exp. Med.* **209**, 807–817 (2012).
40. Yvan-Charvet, L. *et al.* ATP-binding cassette transporters and HDL suppress hematopoietic stem cell proliferation. *Science* **328**, 1689–1693 (2010).
41. Lerch, P.G., Spycher, M.O. & Doran, J.E. Reconstituted high density lipoprotein (rHDL) modulates platelet activity *in vitro* and *ex vivo*. *Thromb. Haemost.* **80**, 316–320 (1998).
42. Murphy, A.J. *et al.* High-density lipoprotein reduces the human monocyte inflammatory response. *Arterioscler. Thromb. Vasc. Biol.* **28**, 2071–2077 (2008).

## ONLINE METHODS

**Reagents.** Ultrapure LPS (*E. coli* 0111:B4), $Pam_3CSK_4$ (P3C) and R848 were from Invivogen. Phosphorothioate backbone–modified CpG DNA oligonucleotides (referred to as CpG) were synthesized by Metabion. Mouse TLR9 stimulatory CpG DNA type B 1826 (5′-TCCATGACGTTCCTGACG TT-3′) and human TLR9 stimulatory CpG DNA type A 2216 (5′-GGGGGAC GATCGTCGGGGGG-3′) were used. Anti–phospho-p65 NF-κB (3033, 1:500 dilution), anti-phospho-p38 MAP kinase (4511, 1:500 dilution), anti-phospho-SAPK/Jnk (4668, 1:500 dilution) and anti–IκB-α (4814, 1:250 dilution) were from Cell Signaling Technology. Anti-IL-1β (BAF401, 1:50 dilution) and anti-IL-6 (BAF406,1:50 dilution) were from R&D systems. Anti-ATF3 (C19; sc-188, 1:50 to 1:200 dilution) was from Santa Cruz and anti-PARP (C2-10; 4338,1:500 dilution) was from Trevigen. Anti-β-tubulin (926-42211,1:1,000 dilution), anti-α-tubulin (926-42213, 1:1,000 dilution), anti-β-actin (926-42210,1:1,000 dilution) and secondary antibodies anti-mouse (926-32212, 1:15,000 dilution), anti-rabbit (926-32213, 1:15,000 dilution) and anti-goat (926-3214, 1:15,000 dilution) were from LI-COR Biosciences. Bovine serum albumin (BSA), actinomycin-D and cyclohexamide were purchased from Sigma.

**Generation of reconstituted HDL.** A reconstituted form of HDL (CSL-111, referred to as 'HDL') with a protein to phospholipid ratio of 1:160, was generated as described previously[43] and provided by CSL Behring.

**Generation of native HDL from human donors.** Native HDL from sera of human donors was purified using a stepwise ultracentrifugation within a density of 1.063–1.21 g/ml as described previously[44]. The distribution and chemical composition of separated lipoproteins in human serum was followed by dialysis against PBS. Approval for isolation of native HDL was obtained from Teikyo University Review Board (Tokyo); informed consent was obtained from donors. Alternatively, native HDL was purchased from Meridian Life Science.

**Animal models.** *TLR-induced inflammation and liver injury mouse model.* Eight-week-old C3H/HeJ female mice were injected intraperitoneally (i.p.) with 2 mg of native HDL or 500 μl control filtrate 6 h before i.p. injection of 20 μg CpG DNA and 10 mg D-galactosamine (D-gal). C3H/HeJ mice (*Tlr4* mutant) were used to avoid the effects of potential endotoxin carried in native HDL. Six- to eight-week-old C57BL/6 female mice were injected i.p. with 2 mg reconstituted HDL or 100 μl PBS for 6 h before injection (i.p.) of 20 μg CpG DNA and 10 mg D-gal. Six- to eight-week-old *Atf3*-deficient mice and matched wild-type (WT) mice were injected i.p. with 2 mg reconstituted HDL or 100 μl PBS for 6 h before i.p. injection of 30 μg CpG DNA and 10 mg D-gal. Blood was collected 1 h after injection of CpG DNA plus D-gal and mice were sacrificed after 10 h. At the time of killing, livers were analyzed by haematoxylin and eosin staining and serum was analyzed for ALT with DRI-CHEM4000 from Fujifilm. Cytokines were measured by Bio-Plex assay from Bio-Rad. These animal experiments were performed in accordance with the Teikyo University animal experiments committee of the Teikyo University School of Medicine (Tokyo) and also in accordance with practices approved by Monash Medical Centre animal ethics committee (Monash University) as obligated by the Australian Code of Practice for the care and use of animals for scientific purposes.

*Atherosclerosis mouse model.* Eight-week-old *Apoe*-deficient mice were fed a high-fat diet (1.25% (wt/vol) cholesterol) for 8 weeks. During week 8, mice were injected intravenously (i.v.) two times with HDL (100 mg/kg) or PBS 4 d apart before the animals were killed, and livers were collected for RNA isolation and mRNA analysis by quantitative PCR (qPCR) as described below. These animal experiments were performed with approval from the Landesamt für Natur, Umwelt und Verbraucherschutz North Rhine-Westphalia and in accordance with German animal protection law.

*Carotid injury mouse model.* For carotid artery injury ~12-week-old male WT and *Atf3*-deficient mice were anesthetized with i.p. injection of 150 mg/kg ketaminehydrochloride (Ketanest, Pharmacia) and 0.1 mg/kg xylazinehydrochloride (Rompun 2%, Bayer). A small incision from the cranial apex of the sternum to just below the mandible was made. After careful preparation of an ~6-mm-long segment proximal of the bifurcation, the common carotid artery was electrically denuded. A 4-mm-long lesion was made by applying two serial 5-s bursts of 2 watts using 2-mm-wide forceps. The skin was then sutured, and the mice were allowed to recover in individual cages before they were returned to their littermates. Three hours later, the mice received a single 200 μl i.v. injection of 20 mg/kg HDL or PBS. After 3 d, 50 μl Evan's blue solution was injected i.v. and allowed to circulate for 5 min. The mice were then killed, and both common carotid arteries fully excised. The arteries were rinsed in 0.9% (vol/vol) NaCl solution, and the residual connective tissue was carefully removed. Images were taken, and the total lesion area (4 mm) and remaining denuded area (stained blue) was measured using AxioVision version 4.5.0 software (Zeiss). The percentage of re-endothelialization was calculated as the difference of blue stained area compared to the total injured area. These animal experiments were performed with approval from the Landesamt für Natur, Umwelt und Verbraucherschutz North Rhine Westphalia and in accordance with German animal protection law.

**Cells.** BMDMs were obtained by culturing bone marrow cells from 6- to 8-week old WT C57BL/6 mice in DMEM supplemented with 10% (vol/vol) FCS, 10 μg/ml Ciprobay-500 and 40 ng/ml M-CSF (R&D Systems). Six days later, BMDMs were collected and plated. Age- and sex-matched WT control mice were used to derive BMDMs for comparative experiments with *Atf3*-deficient BMDMs. Immortalized BMDMs were cultured in DMEM supplemented with 10% FCS and 10 μg/ml Ciprobay-500. Human peripheral blood mononuclear cells (PBMCs) were purified from whole blood over Ficoll density gradient (GE Healthcare); erythrocytes were lysed in red cell lysis buffer (Miltenyi Biotec) and seeded in RPMI supplemented with 10% FCS and 10 μg/ml Ciprobay-500. Human $CD14^+$ monocytes were isolated from PBMCs using CD14 microbeads (Miltenyi Biotec).

**Isolation of Kupffer cells and hepatocytes.** Livers were perfused via the portal vein with a solution of 0.05% (vol/vol) collagenase (Sigma-Aldrich), then mechanically disrupted, filtered through mesh (300 μm) and centrifuged at 300 r.p.m. for 5 min. The hepatocyte cell pellet and the supernatant containing nonparenchymal liver cells were separated and washed once with Hank's Balanced Salt Solution. Nonparenchymal liver cells were labeled with anti-CD11b antibody–labeled MACS microbeads and purified using immunomagnetic separation (Miltenyi).

**Measurement of secreted cytokine levels by ELISA.** Cytokines in cell-culture supernatants were measured by ELISA as per the manufacturer's instructions. Mouse IL-6, IL-12p40 and TNF, and human IL-6 and TNF ELISA kits were from R&D Systems; the human IFN-α ELISA kit was from eBiosciences.

**Cell viability assay.** Cell viability of BMDMs was determined using CellTiter-Blue reagent (Promega) according to the manufacturer's instructions.

**Fast performance liquid chromatography.** Approximately 2 nM of 3′ Alexa Fluor 647–labeled CpG DNA 1826 (Eurofins MWG Operon) or 40 μg of Bodipy-FL–labeled LPS (Invitrogen), were incubated with either PBS or HDL (600 μg) for 2 h at 37 °C. Samples were loaded onto a Superdex-200 size-exclusion column (GE Healthcare), and absorbance was read at 260 nm (RNA/DNA) and 280 nm (protein). Fluorescence absorbance was recorded at 505 nm and 647 nm for LPS and CpG, respectively.

**Quantification of cellular cholesterol.** BMDMs were lysed in 2× RIPA buffer (20 mM Tris-HCl pH 7.4, 150 mM NaCl, 1 mM EDTA, 1% Triton X-100, 10% glycerol, 0.1% SDS and 0.5% deoxycholate), and cholesterol content was measured using the Amplex Red Cholesterol Assay Kit (Invitrogen) according to manufacturer's instructions.

**Cell lysis and immunoblotting.** Up to $1.5 \times 10^6$ BMDMs or $CD14^+$ human monocytes were lysed on ice for 30 min with 1× RIPA buffer (20 mM Tris-HCl pH 7.4, 150 mM NaCl, 1 mM EDTA, 1% Triton X-100, 10% glycerol, 0.1% SDS and 0.5% deoxycholate) supplemented with 0.1 μM PMSF, cOmplete protease inhibitors and PhosSTOP (Roche Biochemicals). Lysates were clarified by centrifugation at 13,000*g* for 10 min at 4 °C and protein concentration measured by BCA assay (Pierce). Equal amount of protein per sample were then run on 4–12% precast SDS-PAGE gels (Novex, Invitrogen) with MES or MOPS

buffer (Novex, Invitrogen). Separated proteins were transferred onto PVDF membranes (Millipore) and blocked in 3% (wt/vol) BSA in Trisbuffered saline with Tween-20 before overnight incubation with specific primary antibodies. Membranes were then washed and incubated with appropriate secondary antibodies, and immunoreactivity was observed by near-infrared detection (Odyssey, LI-COR).

**Preparation of nuclear and cytoplasmic extracts.** Up to $3 \times 10^6$ BMDMs were lysed in cytoplasm lysis buffer (10 mM HEPES pH 7.4, 1.5 M $MgCl_2$ and 10 mM KCl with 0.1% (vol/vol) NP-40) supplemented with 0.1 μM PMSF and cOmplete protease inhibitors (Roche) before intact nuclei were separated from cytoplasmic content by centrifugation at 2,000*g* for 10 min at 4 °C. Supernatants were collected as the 'cytoplasmic extract'. Nuclei were washed with cytoplasm lysis buffer, before being lysed in nuclear lysis buffer (20 mM HEPES pH 7.8, 420 mM NaCl, 20% (vol/vol) glycerol, 0.2 mM EDTA and 1.5 mM $MgCl_2$) and then centrifuged at >13,000*g* for 15 min at 4 °C. The supernatant was then collected as the 'nuclear extract'. Protein content was determined by BCA assay (Pierce). Protein was then subjected to immunoblotting as described above.

**Electromobility shift assay.** Up to $3 \times 10^6$ BMDMs were gently lysed in buffer I (10 mM Tris pH 7.8, 5 mM $MgCl_2$, 10 mM KCl, 1 mM EGTA pH 7, 5% sucrose with DTT, cOmplete protease inhibitors and 0.6% NP-40) and centrifuged at 2,000*g* for 10 min at 4 °C. The nuclei were then lysed in buffer II (20 mM Tris pH 7.8, 5 mM $MgCl_2$, 330 mM KCl and 200 μM EGTA pH 7, 25% glycerol with DTT and protease inhibitors), centrifuged at >13,000*g* for 15 min at 4 °C. The supernatant was then used as 'nuclear extract'. Protein content of the nuclear extract was determined by BCA assay (Pierce), and 5 μg of nuclear extract was incubated with the IRDye-700 NF-κB consensus oligonucleotide (LI-COR) with poly(dI:dC), DTT and NP-40 from the Odyssey EMSA buffer kit as per the instructions. Samples were run on a 4% TBE native polyacrylamide gel, and bands were observed by near-infrared detection (Odyssey, LI-COR).

**Quantification of sterols by mass spectrometry.** Immortalized BMDMs grown in DMEM supplemented with 0.5% FCS and 10 μg/ml Ciprobay-500 were treated with HDL (2 mg/ml) for up to 6 h. Culture supernatants and cells were then subjected to gas chromatography–mass spectrometry–selected ion monitoring (GC-MS-SIM) to determine cholesterol and cholesterol precursor levels as described elsewhere[45,46].

**RNA isolation and generation of cDNA for analysis by SYBR Green quantitative PCR.** Up to $3 \times 10^6$ BMDMs, isolated Kupffer cells, hepatocytes or homogenized tissue samples were lysed and RNA isolated with RNeasy or miRNeasy mini kits according to the manufacturer's protocol (Qiagen). Approximately 1 μg of isolated RNA from each sample was synthesized into cDNA using an oligo $dT_{(18)}$ primer and SuperScript III Reverse Transcriptase (Invitrogen). cDNA abundance was measured by quantitative real-time PCR (qPCR) using the Maxima SYBR Green/ROX qPCR Master Mix (Fermentas) on a 7900T thermocycler (Applied Biosystems). The primer sequences were as follows: mouse *Hprt*, forward 5′-TGAAGTACTCATTATAGTCAAGGGCA-3′ and reverse 5′-CTGGTGAAAAGGACCTCTCG-3′; human *HRPT*, forward 5′-TCAGGCAGTATAATCCAAAGATGGT-3′, and reverse 5′-AGTCTGGCTTATATCCAACACTTCG-3′; mouse *Atf3*, forward 5′-GAGCTGAGATTCGCCATCCA-3′, and reverse 5′-CCGCCTCCTTTTCCTCTCAT-3′; human *ATF3*, forward 5′-CCAACCATGCCTTGAGGATAA-3′, and reverse 5′-GGCAAGGTGCTGAAAATCCTT-3′; mouse *Il6*, forward 5′- CCAGAAACCGCTATGAAGTTCC-3′, and reverse 5′-CGGACTTGTGAAGTAGGGAAGG-3′; mouse *Il12p40*, forward 5′-GGAAGCACGGCAGCAGAATA-3′, and reverse 5′-AACTTGAGGGAGAAGTAGGAATGG-3′; mouse *Il1b*, forward 5′-TTGACGGACCCCAAAAGATG-3′, and reverse 5′-CAGCTTCTCCACAGCCACAA-3′; mouse *Ch25h*, forward 5′-TGACCTTCTTCGACGTGCTG-3′, and reverse 5′-AGCCAAAGGGCACAAGTCTG-3′; mouse *Tnf*, forward 5′-TATGGCCCAGACCCTCACA-3′, and reverse 5′-GGAGTAGACAAGGTACAACCCATC-3′.

Primer specificity was checked by melt-curve analysis. Expression of target genes was normalized to the expression of the housekeeping gene, *HPRT*. For fold change analysis data was transformed using the 'relative standard curve method and comparative threshold cycle (Ct) method (ΔΔCt)' as described by Applied Biosystems.

**RNA isolation for microarray.** Up to $10^7$ cells were lysed in 1 ml of Trizol reagent and stored at −80 °C until further RNA isolation. A total of 0.2 ml chloroform was added to 1 ml of Trizol. The upper colorless aqueous phase was transferred into a new tube after centrifugation. RNA was precipitated by addition of 0.5 ml of isopropyl alcohol with a subsequent washing step in at least 1 ml of 75% ethanol. The precipitated RNA was dissolved in RNase-free water. RNA quality was assessed by measuring the ratio of absorbance at 260 nm and 280 nm using a Nanodrop 2000 Spectrometer (Thermo Scientific) as well as by visualization of the integrity of the 28S and 18S band on an agarose gel.

**Genome-wide transcriptome assessment by microarray.** Total RNA was purified using the MinElute Reaction Cleanup Kit (Qiagen) before array-based gene expression profiling. By using the TargetAmp Nano-g Biotin-aRNA Labeling Kit for the Illumina System (Epicentre), biotin-labeled cRNA was generated. The biotin-labeled cRNA (1.5 μg) was hybridized to MouseWG-6 v2.0 Beadchips (Illumina) and scanned on an Illumina iScan system.

**Data generation and bioinformatics analysis of microarray data.** Processing of raw intensity data was performed by BeadStudio 3.1.1.0 (Illumina). All experiments performed for this study are listed in **Supplementary Table 3.** Data were exported using the Partek report builder and imported as non-normalized data into Partek Genomics Suite V6.6 (PGS) (Partek). Data were then quantile-normalized before further analysis. Differentially expressed genes between the different conditions as well as transcripts with variable expression within the data set were calculated using two- or three-way ANOVA models including batch correction. Differentially expressed genes were defined by a fold change (FC) greater than 2, and a false discovery rate (FDR)-corrected $P < 0.05$ unless stated otherwise. Principle component analysis (PCA) using all transcripts and default settings in PGS was used for visualization of sample relationships. Similarly, default settings within PGS were used for hierarchical clustering to visualize the sample and transcript relationships of the 1,000 most variable genes based on FDR-corrected *P* values in the data set. To link differential gene expression to biological processes involved, GO- and pathway-enrichment analysis were performed in PGS. Furthermore, for visualization of GO enrichment, BINGO (http://www.psb.ugent.be/cbd/papers/BiNGO/Home.html) combined with Enrichment Map (http://baderlab.org/Software/EnrichmentMap/) were used as plugins implemented in Cytoscape (http://www.cytoscape.org/). Heatmaps based on $log_2$-transformed mean expression values were generated using MayDay (http://www-ps.informatik.uni-tuebingen.de/mayday/wp/). To identify potential transcriptional regulators, transcripts differentially expressed between CpG-stimulated BMDMs in the presence or absence of HDL were filtered using the TFCat database[47] and their expression values ($log_2$) visualized as a gene-ranked heatmap.

To predict genes directly targeted by ATF3 after HDL treatment, gene expression experiments were also performed in *Atf3*-deficient BMDMs. This allowed the identification of genes differentially regulated by HDL in WT but not in *Atf3*-deficient BMDMs, as potential direct targets of ATF3 downstream of HDL (**Fig. 6a**). In this model, genes were defined as ATF3 targets if they met the following three criteria: (i) TLR-modified genes being elevated (FC > 1.5) or reduced (FC < −1.5) in expression by stimulation with either CpG or $Pam_3CSK_4$, (ii) TLR-modified genes showing reduced differences (up or down toward control) in the presence of HDL by at least 30%, and (iii) these same genes showing a loss of the HDL effect in *Atf3*-deficient BMDMs.

Gene Set Enrichment Analysis (GSEA; http://www.broadinstitute.org/gsea/index.jsp) was used to determine whether the ATF3 target gene set is statistically significantly enriched in the carotid injury model from HDL-treated WT mice (enrichment score: 0.81; *P* value: 0.0; FDR: 0.0)[48].

**Transcription factor binding prediction.** Transcription factor (TF) binding prediction was performed using the Genomatix software suite (http://www.genomatix.de/) (**Supplementary Fig. 3f**). Briefly, gene symbols of bait genes (most significantly downregulated genes (FC < −3; FDR-corrected $P < 0.05$, two-way ANOVA model) in BMDMs treated with CpG in the presence of HDL) were uploaded into the Genomatix module 'Gene2Promoter' to determine transcripts and promoters of these gene loci. Using standard settings, promoter sequences were compiled as a new sequencing file and further interrogated with the Genomatix module 'common TF sites' to determine TFs





doi:10.1038/ni.2784

with enriched binding sites in the promoters of the chosen gene loci. For the 33 genes, 108 promoter models (104 sequences, 70,162 base pairs (bp)) were identified by Genomatix search for common TF sites in multiple sequences and chosen for further analysis. Nine TF families representing 143 TF candidates revealed TF binding sites in at least 80% of the included promoter models. TF candidates were interrogated for expression as well as differential expression using the comparison of the transcriptome data (131/143 TFs covered) derived from BMDMs treated with CpG either in the presence or absence of HDL. Next, the percentage of expressed genes within the transcriptome data set (23/131, 17.5%) was determined. Among those TFs, ATF3 was the only TF upregulated (FC, 2.3) in macrophages stimulated with CpG in the presence of HDL (**Fig. 3e**). As a second approach, TF modules on the 108 promoter models were computed using Genomatix FrameWorker, which is designed to extract a common framework of elements from a set of TF binding sites. As search criteria, TF modules containing CREB (containing ATF3) or ETSF (containing PU.1) binding sites were given. A total of 80 sequences, from 30 gene loci with 51,851 bp were interrogated. Significantly enriched ($P < 0.03$) module hits ($n = 27$) were identified covering 26/30 genes. The Genomatix module 'Model inspector' was used to assess the location of the generated TF modules. The large majority of hits contained combined CREB-ETFS (69%) modules, with the ETSF family containing the macrophage lineage TF PU.1 (Sfpi1). Calculation of the percentage of gene loci covering CREB-ETSF TF modules was performed in Excel (Microsoft).

**ATF3 ChIP-seq.** ChIP for ATF3 was performed using the EZ-Magna ChIP G Kit (Millipore) according to the manufacturer's instructions. In brief, three biological replicates of BMDMs from WT and *Atf3*-deficient mice were treated with HDL, CpG, HDL then CpG or left untreated. Cells were then cross-linked with 1% paraformaldehyde, before they were lysed and chromatin was sheared by sonication for 30 min with the Covaris S220. Immunoprecipitation was performed over night at 4 °C using 2.5 μg of rabbit polyclonal anti-ATF3 antibody (C-19X, Santa Cruz). After washing, eluted samples were reverse cross-linked and treated with RNase A and proteinase K per the manufacturer's recommendations. ChIP fragments were ligated to NEXTflex ChIP-Seq barcode adaptors using the NEXTflex ChIP-Seq Kit (both BioO Scientific). Adaptor ligated DNA fragments were size-selected (150–250 bp), PCR-amplified, further size selected (150–250 bp), pooled and sequenced on an Illumina HiSeq-1000 sequencer according to the manufacturer's instructions.

**ChIP-seq analysis.** Reads were aligned to the University of California Santa Cruz (UCSC) mm9 reference mouse genome, using Bowtie 0.12.8 (ref. 49). After ChIP-seq quality control using HOMER v4.2 (http://biowhat.ucsd.edu/homer/)[50], reads of biological replicates were pooled, and peak identification was performed using MACS 1.4.2 with the samples from *Atf3*-deficient BMDMs set as unspecific background to identify specific ATF3 binding[51]. Afterward, HOMER v4.2 was used to annotate the genomic location of identified peaks. To generate histograms for the distribution of tag densities, position-corrected tags in 5-bp windows were normalized using Java genomics toolkit (http://palpant.us/java-genomics-toolkit/) and tags from the *Atf3*-deficient BMDMs were subtracted from tags from WT BMDMs. For visualization, only enrichment in WT cells is depicted. Tag coverage of HDL-specific peaks relative to genomic transcription start sites was calculated for WT and *Atf3*-deficient BMDMs for all conditions using HOMER v4.2.

**Statistics.** Data are typically presented as mean values ± s.e.m, where $P < 0.05$ was considered significant as determined by a unpaired two-tailed Student's *t* test, or as described in individual figure legends. Variance was assessed and similar between groups/samples compared in all cases. Analyses were performed with Excel (Microsoft), Prism (GraphPad Software, Inc.) or, for microarray data, with Partek Genomics Suite (Partek) using ANOVA models. All cell culture experiments requiring statistical analysis were performed at least 3 times. For animal experiments requiring statistical analysis we used at least 5 mice per group. No specific method of randomization was used for generation of samples or in animal experiments. Mice (3–5 siblings per cage) were housed according to gender during experiments. Animal models were not performed in a blinded fashion, and the mice were assigned arbitrary numbers during experimentation.


43. Lerch, P.G., Fortsch, V., Hodler, G. & Bolli, R. Production and characterization of a reconstituted high density lipoprotein for therapeutic applications. *Vox Sang.* **71**, 155–164 (1996).
44. Havel, R.J., Eder, H.A. & Bragdon, J.H. The distribution and chemical composition of ultracentrifugally separated lipoproteins in human serum. *J. Clin. Invest.* **34**, 1345–1353 (1955).
45. Thelen, K.M., Laaksonen, R., Paiva, H., Lehtimaki, T. & Lutjohann, D. High-dose statin treatment does not alter plasma marker for brain cholesterol metabolism in patients with moderately elevated plasma cholesterol levels. *J. Clin. Pharmacol.* **46**, 812–816 (2006).
46. Crameri, A. *et al.* The role of seladin-1/DHCR24 in cholesterol biosynthesis, APP processing and Abeta generation in vivo. *EMBO J.* **25**, 432–443 (2006).
47. Fulton, D.L. *et al.* TFCat: the curated catalog of mouse and human transcription factors. *Genome Biol.* **10**, R29 (2009).
48. Subramanian, A. *et al.* Gene set enrichment analysis: a knowledge-based approach for interpreting genome-wide expression profiles. *Proc. Natl. Acad. Sci. USA* **102**, 15545–15550 (2005).
49. Langmead, B., Trapnell, C., Pop, M. & Salzberg, S.L. Ultrafast and memory-efficient alignment of short DNA sequences to the human genome. *Genome Biol.* **10**, R25 (2009).
50. Heinz, S. *et al.* Simple combinations of lineage-determining transcription factors prime cis-regulatory elements required for macrophage and B cell identities. *Mol. Cell* **38**, 576–589 (2010).
51. Zhang, Y. *et al.* Model-based analysis of ChIP-Seq (MACS). *Genome Biol.* **9**, R137 (2008).

Speaking the same language: The World Allergy Organization Subcutaneous Immunotherapy Systemic Reaction Grading System. J Allergy Clin Immunol. 2010;125(3):569-74, 574 e561-74 e567.
5. Paniagua MJ, Bosque M, Asensio O, Larramona H, Marco MT. Immunotherapy with acarus extract in children under the age of 5 years. Allergol Immunopathol. 2002;30(1):20-4.
6. Schubert R, Eickmeier O, Garn H, Baer PC, Mueller T, Schulze J, Rose MA, Rosewich M, Renz H, Zielen S.. Safety and immunogenicity of a cluster specific immunotherapy in children with bronchial asthma and mite allergy. Int Arch Allergy Immunol. 2009;148(3):251-60.
7. Garde J, Ferrer A, Jover V, Pagan JA, Andreu C, Abellan A, Félix R, Milán JM, Pajarón M, Huertas AJ, Lavín JR, de la Torre F. Tolerance of a Salsola kali extract standardized in biological units administered by subcutaneous route. Multicenter study. Allergol Immunopathol. 2005;33(2):100-4.
8. Guardia P, Moreno C, Justicia JL, Conde J, Cimarra M, Díaz M, Guerra F, Martínez-Cócera C, Gonzalo-Garijo MA, Pérez-Calderón R, González-Quevedo T, Sánchez-Cano M, Vigaray J, Acero S, Blanco R, Martín S, de la Torre F.. Tolerance and short-term effect of a cluster schedule with pollen-extracts quantified in mass-units. Allergol Immunopathol. 2004;32(5):271-7.
9. García-Catalán M, Cruz M, Bosque M, Larramona H, Asensio O, Grau R. Safety of a cluster-immunotherapy with a depot allergoid in pediatric patients. Allergy. 2008. 63(88):158-611. A649.
10. Cox L. Accelerated immunotherapy schedules: review of efficacy and safety. Ann Allergy Asthma Immunol. 2006;97(2):126-137; quiz 137-140, 202.

*Manuscript received June 8, 2012; accepted for publication, August 23, 2012.*

**Montserrat Bosque**
Pediatric Allergology and Pneumology Unit
Hospital de Sabadell – Fundació Universitària
Parc Taulí Universitat Autònoma de Barcelona
Parc Taulí 1, 08208 Sabadell, Barcelona, Spain
E-mail: mbosque@tauli.cat

## Novel Mutation of *IL2RG* Gene in a Korean Boy With X-linked Severe Combined Immunodeficiency

YW Lee,[1] EA Yang,[1] HJ Kang,[2] X Yang,[3] N Mitsuiki,[4,5] O Ohara,[4,6] T Miyawaki,[3] H Kanegane,[3] JH Lee[1]
[1]*Department of Pediatrics, Chungnam National University School of Medicine, Daejeon, Korea*
[2]*Department of Pediatrics, Cancer Research Institute, Seoul National University College of Medicine, Seoul, Korea*
[3]*Department of Pediatrics, Graduate School of Medicine and Pharmaceutical Sciences, University of Toyama, Toyama, Japan*
[4]*Department of Human Genome Research, Kazusa DNA Research Institute, Kisarazu, Chiba, Japan*
[5]*Division of Pediatrics and Developmental Biology, Tokyo Medical and Dental University Graduate School, Tokyo, Japan*
[6]*Laboratory for Immunogenomics, Research Center for Allergy and Immunology, RIKEN Yokohama Institute, Yokohama, Japan*

Key words: XSCID. IL-2 receptor. Mutation. Wheezing.

Palabras clave: XSCID. Receptor IL-2. Mutación. Sibilancias.

Severe combined immunodeficiency (SCID) represents a group of rare, sometimes fatal, genetic disorders in which the adaptive immune system is impaired. X-linked SCID (X-SCID) occurs in approximately 50% of patients with SCID and is immunologically characterized by markedly diminished numbers of T cells and natural killer (NK) cells and normal or slightly increased numbers of dysfunctional B cells ($T^-B^+NK^-$ SCID) [1]. Affected patients have a profound deficiency of both cellular and humoral immunities [2,3]. X-SCID is mapped to the Xq13.1 locus and is caused by mutations in the *IL2RG* gene encoding the interleukin 2 receptor (IL-2R) γ chain (common γ chain), which is also associated with cytokine receptors for IL-4, IL-7, IL-9, IL-15, and IL-21 [4]. Therefore, cytokine signaling through the common γ chain is impaired in patients with X-SCID, leading to the impaired development of T and NK cells [4]. Various types of mutation in the *IL2RG* gene have been described in patients with X-SCID. We describe the case of a 5-month-old Korean male with X-SCID who had a novel mutation in the *IL2RG* gene.

A 5-month-old male infant with recurrent bronchiolitis was referred to Chungnan National University Hospital. His weight was 6.3kg (fifth percentile) and his height was 63.9 cm (25th percentile). The patient was born at 39 weeks of gestation after a normal pregnancy and delivery; however, his birth weight was 2.2 kg and there had been intrauterine growth retardation. There was no history of consanguinity in the family. His family history disclosed that 2 maternal uncles had died of infection during the first year of life. From the age of 3 months, the patient had frequently visited and had been admitted to a primary hospital because of recurrent bronchiolitis.

Physical examination on admission showed an emaciated infant with an otherwise normal appearance. The patient had undergone regular scheduled vaccinations until the age of 2 months (BCG, diphtheria-tetanus-acellular pertussis, polio-first shot, hepatitis B virus-second shot), but had not been vaccinated thereafter. He had a BCG scar, but no lymphadenopathy, organomegaly, or skin rash. Rales and expiratory wheezing were positive on auscultation. Human respiratory syncytial virus A antigen was detected in the tracheal aspirated fluid. Computed tomography of the chest revealed bronchial wall thickening with no apparent thymus. The blood counts on admission included white blood cells of 6630/μL (49.3% neutrophils and 35.6% lymphocytes), hemoglobin of 13.1 g/dL, and platelets of 384 000/μL. The patient had absolute lymphopenia (2360/uL). Further investigation demonstrated hypogammaglobulinemia (immunoglobulin [Ig] G, 109mg/dL; IgM,10 mg/dL; IgA, 1mg/dL, and IgE, 0.1 IU/mL) with marked reduction of T cells and NK cells and an increased percentage of B cells (94.3%). Proliferative responses of peripheral blood cells to mitogens were markedly decreased. These results implied $T^-B^+NK^-$ SCID. On the basis of the family history, recurrent infections, absence of thymus, failure to thrive, and deficiency of cellular and humoral immunity, X-SCID was suspected.

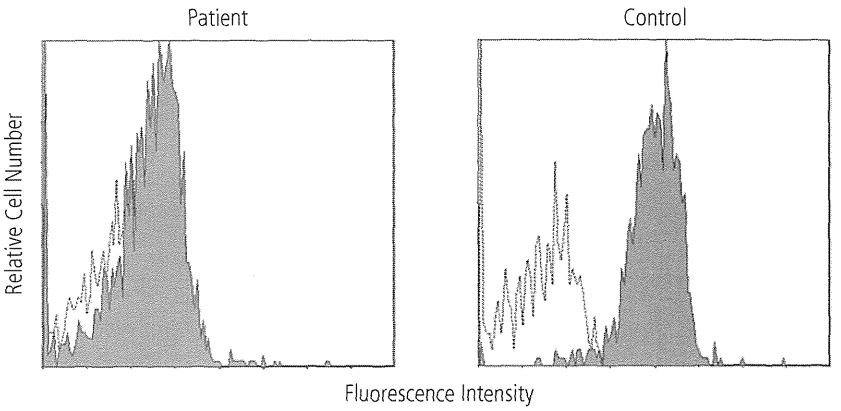


Figure. Interleukin 2 receptor γ (CD132) expression in $CD20^+$ B cells from the patient and a healthy control. Cells were incubated with phycoerythrin-conjugated anti-CD132 monoclonal antibody (clone: TUGh4) and fluorescein isothiocyanate-conjugated anti-CD20 monoclonal antibody, and were analyzed using a flow cytometer. The dotted lines represent the negative control stained with isotype control antibody. The filled areas represent CD132-specific staining.

Blood samples were obtained from the patient and his mother following informed consent. Flow cytometry demonstrated deficient expression of the IL-2R γ chain (CD132) on $CD20^+$ B cells in the patient, indicating IL-2R γ chain deficiency or X-SCID (Figure). The 8 exons and surrounding genomic sequences of the *IL2RG* gene were amplified from genomic DNA as previously described and directly sequenced [5]. A single base insertion at exon 6 (854insG), which resulted in a frameshift mutation (Thr286AspfsX1), was detected in the patient. His clinical course was complicated by recurrent regurgitation, diarrhea, acute suppurative otitis media, and persistent bronchiolitis. At the age of 8 months, he underwent cord blood stem cell transplantation without conditioning at Seoul National University Hospital. The posttransplant course was complicated by grade 1 graft versus host disease of the skin, and the disease responded to prednisolone. However, the patient died of treatment-related complications 1 month after transplantation.

We identified a novel mutation of the *IL2RG* gene in a Korean infant with X-SCID. The patient showed classical clinical features and laboratory data, such as absolute lymphopenia, low percentages of T cells and NK cells, and an increased number of B cells. He was found to have a single nucleotide (guanine) insertion at position 854+1 (854insG) within exon 6, resulting in a frameshift amino acid change. No mutations have been identified at position 854 in the *IL2RG* gene, although many different mutations involving other nucleotide positions in exon 6 have been confirmed. This may be the second genetically identified case of X-SCID in Korea. The first patient showed a single point mutation (C690T) with a missense mutation (R226C), which has been previously reported in many ethnic backgrounds[6]. A total of 344 mutation entries, comprising 198 unique molecular events, are now present in the X-linked SCID mutation database (IL2RGbase) (http://research.nhgri.nih.gov/scid/). Many types of mutation have been reported throughout all 8 exons of the *IL2RG* gene.

In conclusion, we have reported a novel mutation of the *IL2RG* gene in a patient with X-SCID. A diagnosis of SCID should be suspected in patients with persistent infection and absolute lymphopenia in early infancy, as occurred in our patient. We believe we might have reported the second case of X-SCID and the third case of SCID including IL-7Rα chain deficiency in Korea [7]. There may be more Korean patients with SCID. Further studies of X-SCID in this country are needed to clarify the differences observed in mutations and disease between different ethnic groups. Neonatal screening of the measurement of the T cell receptor excision circle is useful for detecting patients with SCID and severe T lymphopenia[8]. This method has been applied in some states in the United States, and it may be applicable in Korea.

## Acknowledgments

This study was partly supported by the Basic Science Research Program through the National Research Foundation of Korea (NRF) funded by the Ministry of Education, Science and Technology (2011-0021633) and Grants-in-Aid for Scientific Research from the Ministry of Education, Culture, Sports and Technology and grants from the Ministry of Health, Labor and Welfare of Japan. We thank Ms Chikako Sakai and Mr Hitoshi Moriuchi for their technical assistance.